THE ROLES OF ACTIVIN A AND B IN LIVER INFLAMMATION AND FIBROSIS

by

Matthew J. Hamang

A Thesis

Submitted to the Faculty of Purdue University

In Partial Fulfillment of the Requirements for the degree of

Master of Science

Department of Biological Sciences

Indianapolis, Indiana

May 2019

THE PURDUE UNIVERSITY GRADUATE SCHOOL
STATEMENT OF COMMITTEE APPROVAL

Dr. Guoli Dai, Chair

Department of Biology

Dr. James Marrs

Department of Biology

Dr. Benjamin Yaden

Department of Biology

Approved by:

Dr. James Marrs

Head of the Graduate Program

Dedicated to Karen

ACKNOWLEDGEMENTS

The author would like to thank those who provided assistance in generating the work presented here - in alphabetical order Alex Culver, Brandy Snider, Yan Wang, and Daniel Xu. In particular, I would like to express many thanks to Dr. Dai, Dr. Marrs, and Dr. Yaden for the opportunity to pursue this degree and for their guidance and mentorship throughout the process. I would also like to thank Dr. Henry Bryant and Dr. Yanfei Ma for their support and finally Dr. Masahiko Sato for kindling my passion for science and helping to launch my career many years ago.

TABLE OF CONTENTS

LIST OF TABLES

LIST OF FIGURES

LIST OF ABBREVIATIONS

AICD	Activation-induced cell death
ActRIIB-Fc	Ectodomain of ActRIIB and Fc-region of immunoglobulin
ALK	Anaplastic lymphoma kinase
ALT	Alanine aminotransferase
AST	Aspartate aminotransferase
APC	Antigen presenting cell
BCR	B-cell receptor
BQL	Below quantifiable limit
CCl_4	Carbon tetrachloride
CTGF	Connective tissue growth factor
CTL	Cytotoxic T-cell
DC	Dendritic cell
ECM	Extracellular matrix
GS	Glycine- and serine-rich sequence
HCC	Hepatocellular carcinoma
HSC	Hepatic stellate cell
IFN-γ	Interferon gamma
KC/GRO	Keratinocyte chemoattractant/growth-regulated oncogene
LPS	Lipopolysaccharide
MHC	Major histocompatibility complex
MMP	Matrix metalloproteinase
MTS	Masson's trichrome staining

NASH	Nonalcoholic steatohepatitis
NAFLD	Nonalcoholic fatty liver disease
NK	Natural killer
NKT	Natural killer T
PDGF	Platelet-derived growth factor
qNMR	Quantitative nuclear magnetic resonance
SARA	SMAD anchor for receptor activation
STAT	Signal transducer and activator of transcription
TCR	T-cell receptor
TGFβ	Tissue growth factor beta
TIMP	Tissue inhibitor of metalloproteinse
TNF	Tumor necrosis factor
TLR	Toll-like receptor

ABSTRACT

Author: Hamang, Matthew, J. MS
Institution: Purdue University
Degree Received: May 2019
Title: The Roles of Activin A and B in Liver Inflammation and Fibrosis
Committee Chair: Guoli Dai

Liver fibrosis is the result of different types of chronic liver diseases, such as cholestatic liver disease and nonalcoholic steatohepatitis, among others. Fibrosis, if left unchecked, may progress to the point of cirrhosis – permanently affecting liver function detrimentally and potentially leading to development of hepatocellular carcinoma. Inflammatory response following tissue injury is vital for the initiation of fibrosis; chronic inflammation results in abnormal tissue healing and promotes a pro-fibrogenic response.

Activins are cytokines that have been identified as members of the TGFβ superfamily of growth and differentiation factors. Activin A and B, in particular, have been identified as having roles in the pathophysiology of liver disease, but have not been investigated thoroughly. We treated mice with concanavalin A, a potent T-cell mitogen with liver specificity when administered intravenously, and characterized the resulting response to liver injury and how activin A and B are modulated during this acute inflammatory phase. We showed that activin B is highly increased in circulation following inflammation, as well as locally in the liver as well as the spleen. We then neutralized activin A and B via neutralizing antibodies in our concanavalin A-induced liver injury model to determine if inhibition of these ligands may confer protective effects during the acute inflammatory response in liver. Neutralization of either activin A or activin B protected hepatocytes, improved liver function, and significantly reduced circulating cytokines following concanavalin A administration. Finally, we determined whether inhibition

of activin A or B might prevent or reverse the development of liver fibrosis after disease has been established. We induced liver fibrosis in mice via the hepatotoxin carbon tetrachloride, and then treated with neutralizing antibodies while still maintaining carbon tetrachloride administration. Neutralization of activin A and B markedly reduced liver fibrosis, protected hepatocytes, and improved liver function. Our findings implicate both activin A and B as major players in the acute inflammatory response to liver injury, as well as during chronic injury and fibrogenesis, and demonstrate the therapeutic potential of targeting these ligands for the treatment of fibrosis in chronic liver diseases.

CHAPTER 1. LITERATURE REVIEW

1.1 Liver injury and fibrosis

Liver fibrosis is the product of chronic liver damage, in addition to excess accumulation of extracellular matrix (ECM) proteins in the liver, and is characteristic of most types of chronic liver diseases, such as cholestatic liver disease and nonalcoholic steatohepatitis (NASH) [1,2]. In acute liver failure, generally a robust and self-limiting fibrotic and regenerative response occurs [3]. This fibrotic response becomes an issue, however, when dysregulated and excessive scarring occurs in response to persistent injury and alters tissue function [4]. Eventually, if left unchecked, liver fibrosis will progress to the point of liver cirrhosis where damage to the liver is generally regarded as irreversible, and may eventually result in hepatocellular carcinoma (HCC).

Insult or damage to epithelial cells in the liver (either hepatocytes or cholangiocytes) results in the release of inflammatory mediators, leading to the stimulation and activation of hepatic stellate cells (HSCs) which transdifferentiate to become myofibroblast-like cells, characterized by an excessive release of ECM proteins and release of pro-inflammatory and pro-fibrogenic factors including TGFβ [4]. Following damage leukocytes are recruited to the site of injury to phagocytize apoptotic or dead cells and amplify inflammatory response by secreting pro-inflammatory cytokines (including TGFβ), as well as by recruiting additional T-cells [4]. Pro-inflammatory mediators, growth factors, and cytokines (including PDGF, CTGF, TGFβ, and IL-13) from cellular damage and stimulated immune cells activate mesenchymal precursor cells to transdifferentiate to myofibroblasts as well [4,5]. However, mechanisms driving the initiation and progression of liver fibrosis remain elusive.

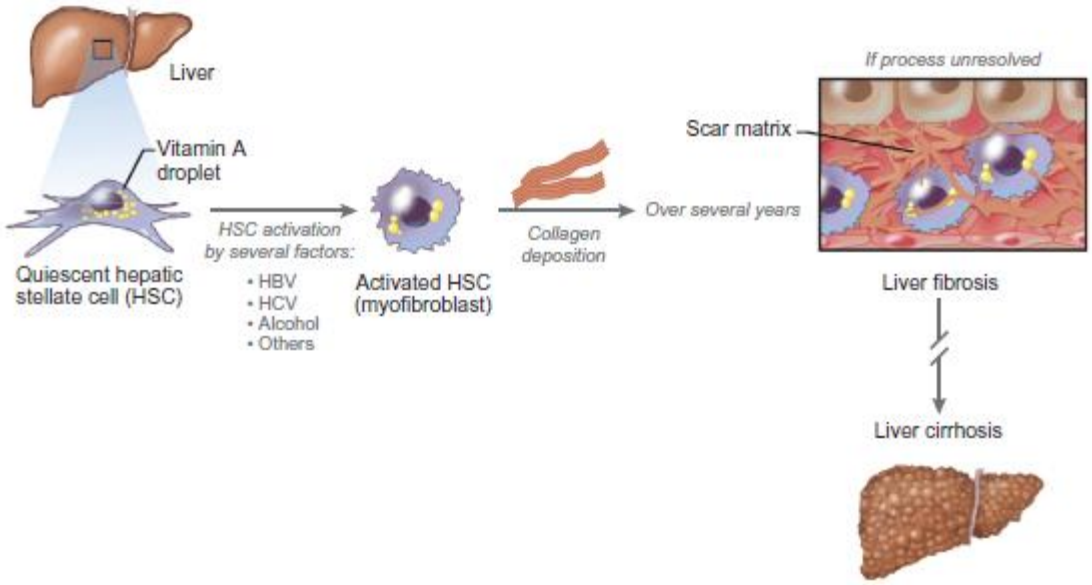

Figure 1-1: Schematic of liver fibrogenesis. **Ismail, *Reversal of hepatic fibrosis: pathophysiological basis of antifibrotic therapies November 2013.***

1.2 Lymphocytes in Immune Responses

Lymphocytes are white blood cells that vary in function and include T, B, and natural killer (NK) cells; T and B cells are the effectors of adaptive immunity, and NK cells lack recombined antigen receptors and are innate immune lymphocytes [6]. Lymphocytes are essential in the immune response to foreign antigen and through continual recirculation between specific sites facilitate both continual immune surveillance, and recognition and response to antigen when it enters the body [7]. During development, lymphocyte lineage and specificity are determined through generation of either T-cell receptor (TCR) for T-cells or B-cell receptor (BCR) for B-cells. NK cells are unique in the fact that they do not express either TCR or BCR, and do not require antibody or major histocompatibility complex (MHC) in order to activate. MHC is a molecule expressed on the surface of all nucleated cells (and platelets) of jawed vertebrates, and is required for priming of naïve T-cells. When T cells encounter MHC bound with antigen on antigen presenting cells (APCs) such as dendritic cells (DC) or macrophages, TCR signals result

in changes in adhesion molecules to promote continued binding of the two cells which allows for costimulatory signaling though CD28 (on the T-cell) and B7-1/2 (also known as CD80/86) (on the APC) in CD8+ cells. In CD4+ cells, the costimulatory signaling is through CD40L (on the T-cell) and CD40 (on the APC). Priming of naïve CD8+ T-cells (which bind MHCI expressed on all nucleated cells and platelets) results in cytotoxic T-cells (CTL), which can directly kill pathogen-infected cells through the release of perforin, granzymes, and granulysin - which lead to a cascade of events that trigger apoptosis in the target cell. Primed CD4+ cells (which bind MHCII expressed on professional APCs such as B-cells, dendritic cells, and mononuclear phagocytes) develop into a diverse array of effector cell types that express specific master transcription factors depending on cytokines generated from innate cells during the priming process as well as the strength of the antigenic stimulation [8].

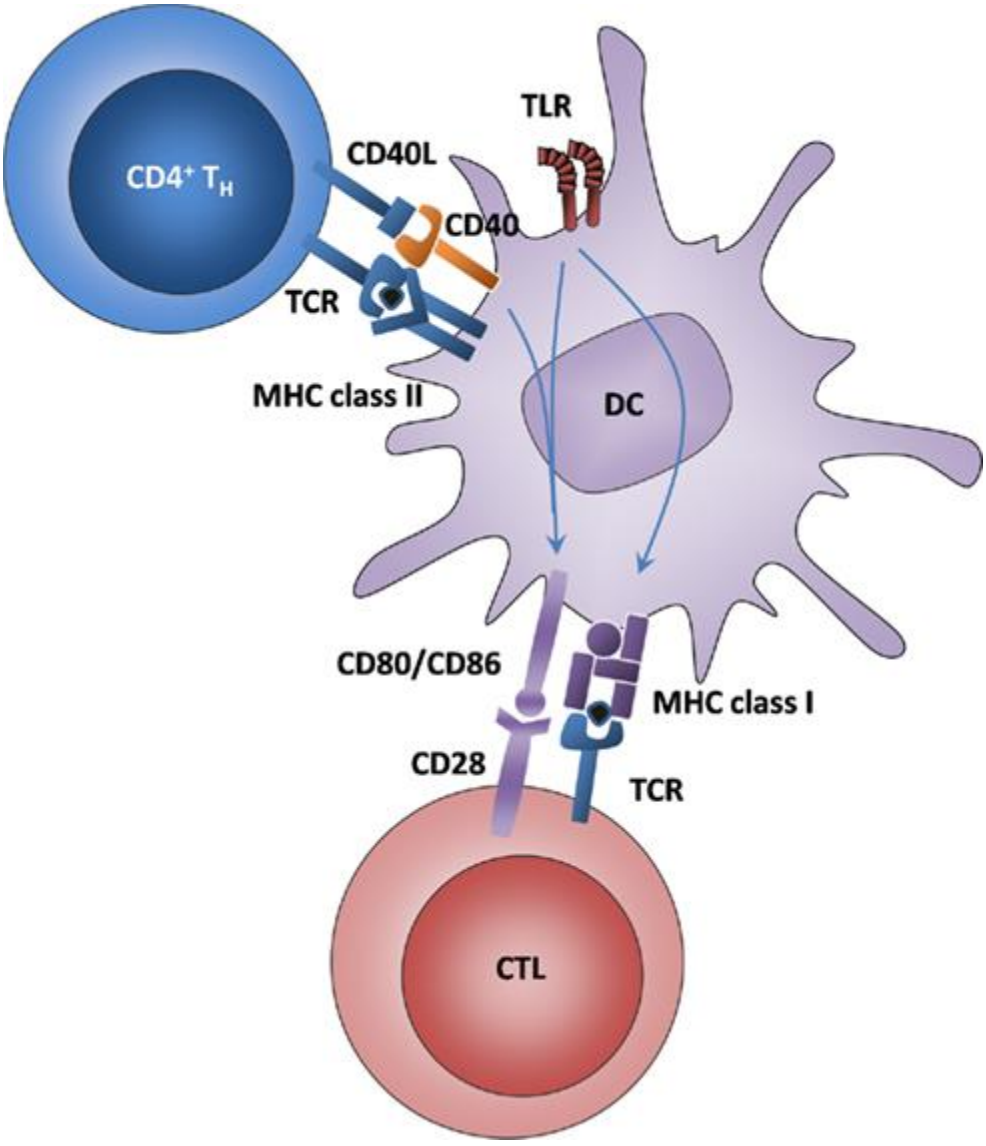

Figure 1-2: CD4+ and CD8+ T-cell signaling. **Thaiss*, Chemokines: a new dendritic cell signal for T cell activation August 2011*.**

1.3 Immune cells in liver injury and fibrosis

Regarding fibrosis in the liver, many of the cells involved in the innate immune response may only have a minimal effect on tissue fibrosis [9]. In fact, NK cells have been shown to actively suppress fibrosis by termination of activated myofibroblasts through TRAIL dependent mechanisms [10]. Macrophages, however, are responsible for both the progression and resolution of fibrosis in the liver. Macrophages contribute to the initiation of fibrogenesis through

production of TGFβ1 and insulin-like growth factor, which promotes fibroblast expression to start matrix remodeling [11]. Additionally, macrophages have been shown to produce IL-6 and TGFβ, which leads to maintenance of proliferation and differentiation in fibroblasts [12]. Macrophages follow two distinct patterns of activation and polarization following stimulation. Following stimulation with Toll-like receptor (TLR) ligands, IFN-γ (produced by Th1 cells and NK cells) and TNF (produced by APC cells) macrophages undergo classical activation (becoming M1 macrophages) [13]. These macrophages are characterized by secretion of multiple pro-inflammatory cytokines (IFN-γ, IL-1, IL-6, IL-12, IL-23 and TNFα) and are associated with Th1 lymphocyte response and cell-mediated immunity [9]. Macrophages may also undergo alternative activation, becoming M2 macrophages. This activation profile is a Th2 polarized response characterized by STAT-6 signaling, secretion of IL-4 and IL-13, and upregulation of endocytic lectin receptors [9]. M2 macrophages are generally associated with resolution of inflammation (through production of immunosuppressive IL-10) or wound healing (through production of IL-4 and upregulation of arginase, the enzyme associated with production of polyamides and collagen) [14].

The human liver contains a significant number of resident lymphocytes (~10^{10} cells), which are comprised of both adaptive lymphocytes (B cells, CD4+ cells, and CD8+ cells) as well as innate lymphocytes (NK and NKT cells) [15]. Depletion of either T-cells or B-cells have been shown to have protective effects from fibrosis in the liver [16,17]. Additionally, $RAG2^{-/-}$ mice deficient in both T and B-cells show resistance to fibrosis in acute and chronic models of liver injury [17]. The interaction of T helper cells during acute and chronic inflammation drives the polarity of the response, and different expression profiles result from the cytokines produced by either Th1 or Th2 cells. Generally, cytokines produced by Th1 cells (such as IFN-γ, IL-2, and TNFC) are

associated with an intense cellular response through cell-mediated immunity and phagocyte-dependent inflammation [18]. Th2 cytokines, on the other hand, increase the expression of several pro-fibrogenesis genes including pro-collagen I and III, MMP2, MMP9 and TIMPs [12]. Blocking receptor for IL-13 signaling, a pro-fibrosis cytokine produced by Th2 cells [19], has been shown to reduce liver fibrosis [20]. Additionally, using targeted mutations to disrupt IL-4 and its receptor, as well as STAT6 also attenuate liver fibrosis in mice [21]. Regarding cytotoxic T-cells - transfer of CD8+ cells, but not CD4+ cells, from mice with liver fibrosis induced by CCl_4 treatment into immune compromised SCID mice results in significant liver injury [16]. In the context of fibrosis in the liver, CD4+ cells are responsible for local production of cytokines that promote fibrogenesis by affecting macrophages and fibroblasts, while CD8+ cells promote local tissue injury by releasing pro-inflammatory cytokines that may indirectly lead to fibrosis [9].

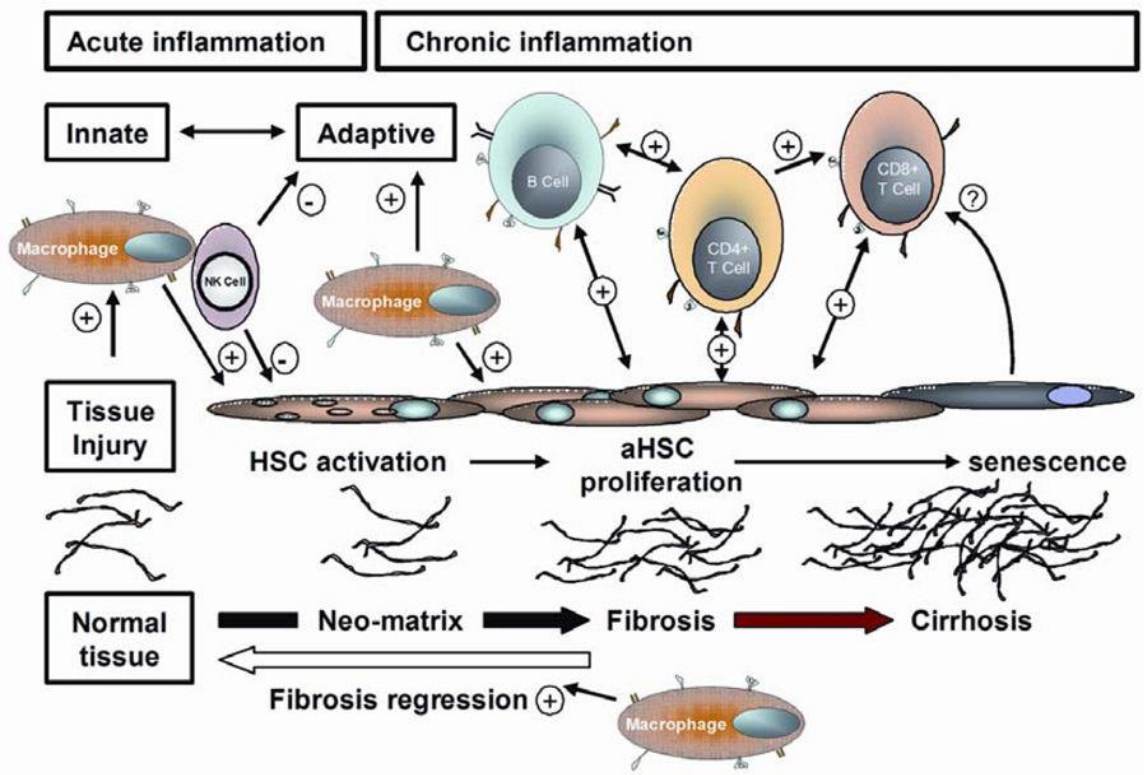

Figure 1-3: Interactions of the innate and adaptive immune systems in liver fibrosis. **Holt, *Immune interactions in hepatic fibrosis. or "Leucocyte-stromal interactions in hepatic fibrosis" November 2018.***

1.4 Activin A and B in liver injury and fibrosis

Activins are a group of cytokines classified under the TGFβ superfamily of growth and differentiation factors [22], like TGFβ, are formed via the covalent dimerization of two subunits [23]. In humans and other mammals, four subunits of activin have been identified: beta A, beta B, beta C and beta E. Of all of these subunits – A, B, and C have been found in humans, and A, B, C, and E in mouse. Activin A is the homodimer of two beta A subunits, and activin B is the homodimer of two beta B subunits. Activin has both a type I and type II receptor which both contain a short extracellular domain that binds ligand, and a larger intracellular serine/threonine kinase domain [24]. The type II receptor (ActR-II or ActR-IIB) is constitutively active, and will dimerize and bind activin A and B first [24]. Afterwards, the bound type II receptors will recruit a

type I receptor (ActR-IA/B) each and activate them via phosphorylation of the membrane-proximal glycine- and serine-rich sequence (GS) region [25]. When they bind to the same type II receptor, activins A and B recruit ALK7 (ACVR1C) as the type I receptor [26]. Following ligand binding, receptors are internalized [27]; the SMAD anchor for receptor activation (SARA) is a zinc double finger FYVE domain containing protein present in the early endosome which is internalized along with the hetero-tetrameric receptor complex via clathrin-mediated endocytosis [28]. SARA then will recruit a receptor-regulated SMAD (R-SMAD), orienting the R-SMAD so that the serine residue on its C-terminus can bind the catalytic L45 region of the Type I receptor [29]. The type I receptor will then phosphorylate this serine residue of the R-SMAD, inducing a conformational change which allows dissociation of the R-SMAD from the receptor complex and SARA [30]. Activins have been shown to signal through the R-SMADS SMAD 2 and SMAD 3 [31]. The dissociated, phosphorylated R-SMAD then binds the common mediator Smad 4 and this complex translocates to the nucleus to regulate gene expression [32].

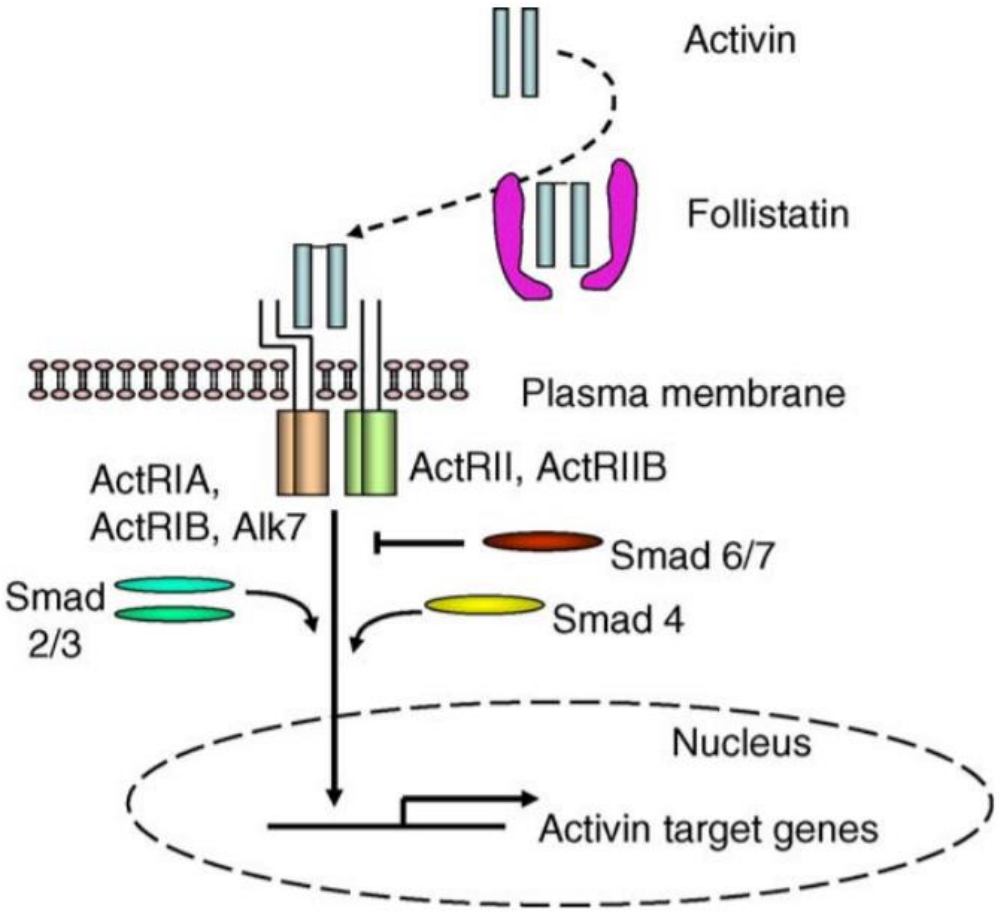

Figure 1-4: Activin receptor signaling. **Werner, *Roles of activin in tissue repair, fibrosis, and inflammatory disease February 2006.***

Activin A has a wide tissue distribution and is produced by numerous cells including macrophages, Th2 cells, and hepatocytes [32–34]. Activin A is an important mediator of liver pathophysiology, through proliferation of hepatocytes, activation of HSCs, secretion of liver extracellular matrix, and the formation and development of liver injury [35]. Activin A expression is significantly elevated in CCl_4-induced chronic liver injury in mice, marking it as a potential regulator of liver fibrosis development [36]. Additionally, activin A protein in serum as well as liver is significantly increased in a mouse model of immune hepatitis and fibrosis, and knockdown of activin A type 2 receptor in this model resulted in significant reductions in ALT and AST (liver enzyme markers of damage), hydroxyproline in liver, and hepatic fibrosis as

measured by Masson trichrome staining [37]. In humans, activin A levels in serum have been shown to be significantly elevated in individuals with non-alcoholic fatty liver disease (NAFLD). In patients with non-alcoholic steatohepatitis (NASH) high levels of activin A are significantly correlated with the degree of hepatic fibrosis [38]. Taken together, these lines of evidence implicate a functional role for activin A in liver homeostasis and disease, which, however, has not been intensively studied.

The function of activin B in the liver is poorly understood [39]. Expression of beta B subunit of activin is low in rodent liver [40], but is detectable by immunohistochemistry at low levels in hepatocytes of normal rat livers and in connective tissue septa in fibrotic livers [41]. In humans, however, beta A and beta B transcripts are expressed at similar levels in liver [42]. Expression of activin beta B mRNA has been shown to be highly upregulated in stellate cells of rat livers following CCL_4 administration [43] and following exposure to peroxisome proliferator di-n-butyl phthalate [44]. Additionally, in a model of lipopolysaccharide (LPS)-induced liver inflammation in mice βB subunit expression levels are significantly increased, but not inhibin α or βA subunit [45]. These data taken together suggest a role for activin B in the pathology of liver inflammation and fibrosis.

CHAPTER 2. MATERIALS AND METHODS

2.1 Animal care and use

All mouse studies were performed with the approval of Eli Lilly and Company's Institutional Animal Care and Use Committee in accordance with the National Institute of Health Guide for the Care and Use of Laboratory Animals. For concanavalin A immune-mediated hepatitis studies, male Balb/c mice were used (Envigo, Indianapolis, IN) at 12 weeks of age. For carbon tetrachloride (CCl_4) induced liver fibrosis, female C57BL/6 mice were used (Envigo, Indianapolis, IN) at 12 weeks of age. Animals were allowed to acclimate for a minimum of 72 hours in a climate controlled room (22±2°C) on a 12-hour light-dark cycle (with lights on at 6:00AM) with ad lib access to water and normal chow (TD2014, Teklad, Madison, WI). Prior to study start, animals were randomized according to body weight.

2.2 Concanavalin A immune-mediated hepatitis

Acute immune-mediated hepatitis was induced by a single intravenous (IV) administration of concanavalin A (MP Biomedical, Solon, OH) dissolved in phosphate-buffered saline (200 μL per animal). For the initial dose-response characterization study, concanavalin A was administered at 10 mg/kg, 15 mg/kg, 20 mg/kg, or 25 mg/kg. For the second study, mouse IgG1 isotype control (50 mg/kg), activin A (10 mg/kg) or activin B (50 mg/kg) neutralizing antibodies (Eli Lilly, Indianapolis, IN) in phosphate-buffered saline were administered subcutaneously (SC) at 16 hours prior to concanavalin A injection, which was administered at 15 mg/kg. 12 hours following concanavalin A administration, mice were sacrificed by CO_2 asphyxiation and blood collected via cardiac puncture and serum separated using MiniCollect Z serum separating tubes (Greiner Bio-one, Kremünster, Australia) . Following blood collection, a secondary method of

euthanasia was performed (cervical dislocation) and liver, gastrocnemius, and spleen were excised and either snap-frozen in liquid nitrogen or fixed in 10% neutral-buffered formalin for histological analysis. Serum and frozen tissues were stored at -80 °C until analyzed.

2.3 CCl_4-induced liver fibrosis

Hepatic fibrosis was induced via intraperitoneal (IP) injections of CCl_4 (1 mL/kg) diluted 1:10 in corn oil twice weekly for 6 weeks. Control animals were given only corn oil following the same dosing regimen as CCl_4-treated mice. After 6 weeks of CCl_4 administration, mouse IgG1 isotype control (60 mg/kg), activin A antibody (10 mg/kg), activin B antibody (50 mg/kg), the combination of both neutralizing antibodies, or soluble activin receptor type IIB (Eli Lilly, Indianapolis, IN) were administered once weekly for 4 weeks. During this 4 week period, CCl_4 was still administered twice weekly at 1 ml/kg. Following 4 weeks of treatment, mice were sacrificed by CO_2 asphyxiation and blood collected via cardiac puncture and processed for serum. Following blood collection, a secondary method of euthanasia was performed (cervical dislocation) and liver, gastrocnemius, and spleen were excised and fixed in 10% neutral-buffered formalin for histological analysis. Serum was stored at -80 °C until analyzed.

2.4 Body composition (quantitative NMR)

In animals treated with CCl_4, quantitative nuclear magnetic resonance (qNMR) imaging was performed at the beginning of the study before CCl_4 administration and after 6 weeks of CCl_4 administration. During the antibody treatment phase, qNMR was performed weekly and prior to study termination. Lean body mass, fat mass, and free water content were measured (qNMR; Echo Medical systems, Houston, TX).

2.5 Biochemical assays

Serum samples were analyzed for aspartate aminotransferase (AST), alanine aminotransferase (ALT), glucose, bile acids, total cholesterol, and total bilirubin levels with a Hitachi Modular Analyzer (Roche Diagnostics, Indianapolis, IN). For concanavalin A studies, serum activin A and activin B protein contents were measured via ELISA according to the manufacturer's protocols (activin A ELISA kit, Sigma, St. Louis, MO; activin B ELISA kit, Ansh labs, Webster, TX). Additionally, for the concanavalin A dose response study, activin A and activin B protein levels were measured in liver and spleen. Tissue lysates were processed using approximately 100 mg of tissue with 1mL of lysis buffer (Cell Signaling Technologies, Dancers, MA), with protease inhibitor added (protease inhibitor tablets EDTA-free; Pierce Biotechnology, Rockford, IL). Total protein concentrations were measured via Bradford assay (Coomassie plus protein assay; Pierce Biotechnology, Rockford, IL) and protein content between tissue samples normalized before performing ELISAs. For the concanavalin A antibody study, serum samples were measured for cytokine levels using V-PLEX Plus Proinflammatory Panel 1 kit (Meso Scale Discovery, Rockville, MD) according to the manufacturer's protocol.

2.6 Histology and immunohistochemistry

For the CCl_4 study, fixed liver samples were processed, paraffin-embedded, and subjected to a standard procedure of immunohistochemistry. Primary antibodies against F4/80 (eBioscience, San Diego, CA), MPO (R&D System, Minneapolis, MN), and Ki67 (Abcam, Cambridge, MA) were used. The liver sections were subjected to Masson's trichrome staining (Abcam, Cambridge, MA) as well. Images were acquired using digital slide scanning (ScanScope XT, Aperio, Vista, CA) and quantification of stained areas performed using ImageJ (National Institutes of Health, NIH, USA).

2.7 Quantitative real-time PCR

mRNA in liver and spleen from the concanavalin A dose response study was isolated by adding 1ml of TRIzol reagent (Ambion, Carlsbad, CA) to tissue samples in lysing matrix D FastPrep tubes (MP Biomedicals, Solon, OH); samples were then homogenized (Fast-Prep96, MP Biomedicals, Solon, OH). The manufacturer's protocol for RNA isolation with TRIzol was followed until phase separation, then aqueous phase was removed and RNA isolated and purified using PureLink Pro 96 purification kit (Invitrogen, Carlsbad, CA). RNA concentration and purity was assessed by measuring sample absorbance at 260/280 nm via Nanodrop (ThermoFisher Scientific, Wilmington, DE). 2 μg of RNA was reverse-transcribed to cDNA using a high capacity cDNA reverse-transcription kit (Applied Biosystems, Forster City, CA) in a 20ul reaction. cDNA was combined with TaqMan Universal Fast Master Mix (Applied Biosystems, Forster City, CA) and TaqMan primer probes (Applied Biosystems, Forster City, CA), and qPCR analysis performed via QuantStudio 7 Flex system (Applied Biosystems, Carlsbad, CA). Threshold values were generated for Inhibin A (Inhba, Mm00434339_m1) and Inhibin B (Inhbb, Mm03023992_m1) in both liver and spleen, and data reported as $2^{-\Delta\Delta Ct}$ relative to control. For liver, the housekeeping gene used was Hprt1 (Hprt, Mm00446968_m1). For spleen, the housekeeping gene used was β-actin (Actb, Mm02619580_g1).

2.8 Data analysis

All data expressed as mean ±SEM. Statistical analysis was performed using GraphPad Prism version 7. Statistical significance (p-value ≤ 0.05) was analyzed by one-way ANOVA.

CHAPTER 3. RESULTS

3.1 Characterization of concanavalin A immune-mediated hepatitis

We evaluated an *in vivo* model of acute hepatitis induced by intravenous concanavalin A administration in mice to explore the relationship between immune system activation during acute inflammation and how activin A and B may be involved. Animals were separated into five groups (n=6) and administered varying doses of concanavalin A (Table 3-1):

Table 3-1 Groups in concanavalin A characterization study

Group Number	Stimulation
1	PBS (200 μL, IV)
2	ConA (10 mg/kg, IV)
3	ConA (15 mg/kg, IV)
4	ConA (20 mg/kg, IV)
5	ConA (25 mg/kg, IV)

Concanavalin A is a plant lectin extracted from the jack-bean (*Canavalia ensiformis*) and when delivered intravenously is a liver-specific T-cell selective mitogen, crosslinking surface glycoprotein located on liver sinusoidal endothelial cells to T-cell receptors on T-cells and Kupffer cells, activating them [46]. In this way the concanavalin A model differentiates itself from other models as insult to liver is highly specific and mediated solely through lymphocyte activation and immune-mediated damage, versus through primary damage to hepatic parenchymal tissue followed by secondary immune-mediated damage (CCL_4 model), or through less tissue-specific innate and adaptive immune responses (LPS mediated) [46]. We anticipated that following concanavalin A immune-mediated damage to hepatocytes would be reflected through increases in serum clinical markers for liver damage (aspartate aminotransferase (AST),

alanine aminotransferase (ALT), total bilirubin, etc.). As response to concanavalin A and cytokine profile will vary based on time from administration, we focused on evaluating the time at which maximum damage to liver is achieved based on increases to clinical markers, which is roughly 12 hours after treatment [43].

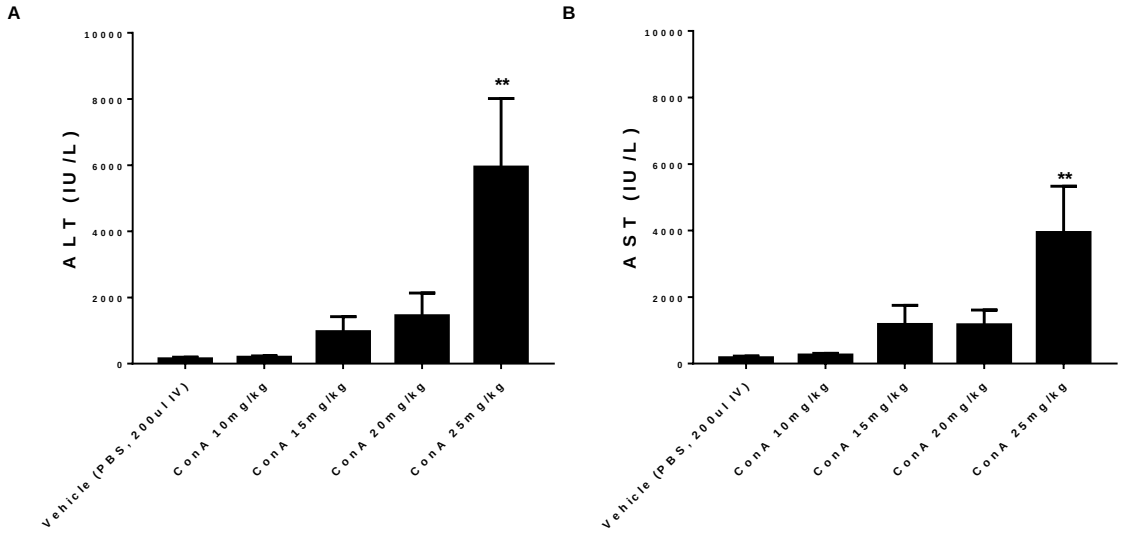

Figure 3-1 Response of ALT and AST to intravenous concanavalin A administration. Lean male Balb/c mice were administered a single dose of concanavalin A intravenously. Serum levels of ALT **(A)** and AST **(B)** were measured from serum collected 12 hours post-dose. Data are expressed as mean ± S.E.M. (n=6 mice/group). Significance is indicated **P ≤ 0.01, treated group versus vehicle control group (Dunnett's one-way ANOVA).

Concanavalin A treatment showed increases in serum ALT and AST starting at 15 mg/kg, reaching highly significant differences compared to vehicle control at 25 mg/kg. Increasing dosage threshold from 20 mg/kg to 25 mg/kg resulted in a substantial increase in both ALT and AST in serum. We also measured total bilirubin and bile acids in serum, which followed the same trend that with increasing dosage of concanavalin A, clinical parameters increased.

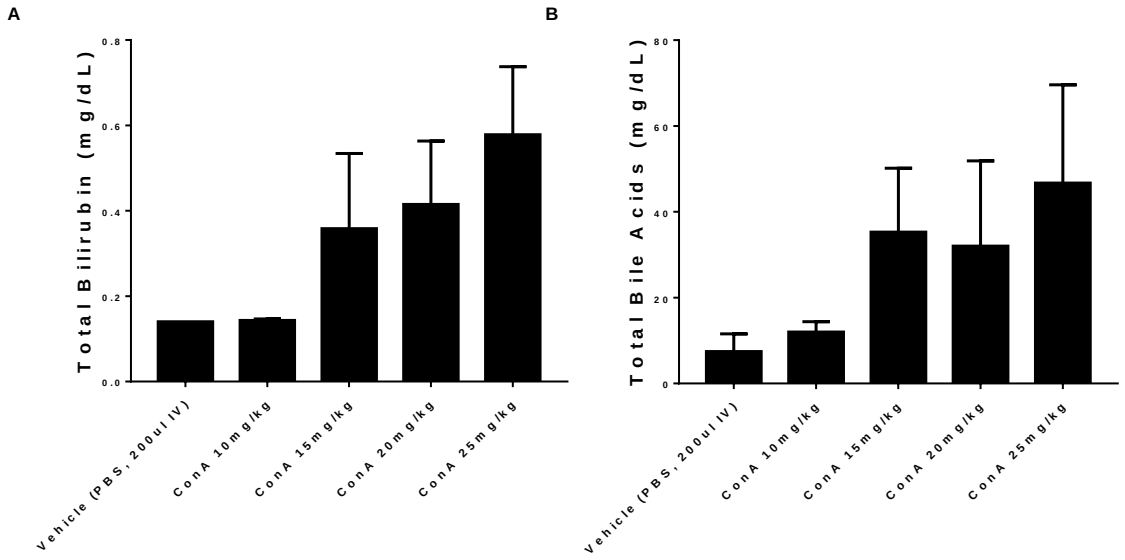

Figure 3-2 Response of bilirubin and bile acids to intravenous concanavalin A administration. Lean male Balb/c mice were administered a single dose of concanavalin A intravenously. Serum levels of bilirubin **(A)** and bile acids **(B)** were measured from serum collected 12 hours post-dose. Data are expressed as mean ± S.E.M. (n=6 mice/group).

Additionally, we also evaluated serum glucose and total cholesterol levels following concanavalin A treatment as liver gluconeogenesis and cholesterol homeostasis and metabolism are negatively impacted following liver injury. We found that with increasing dosage of concanavalin A, blood glucose levels were significantly decreased starting at 15mg/kg and steadily decreased throughout increasing dosage. There were no significant effects on circulating cholesterol in serum.

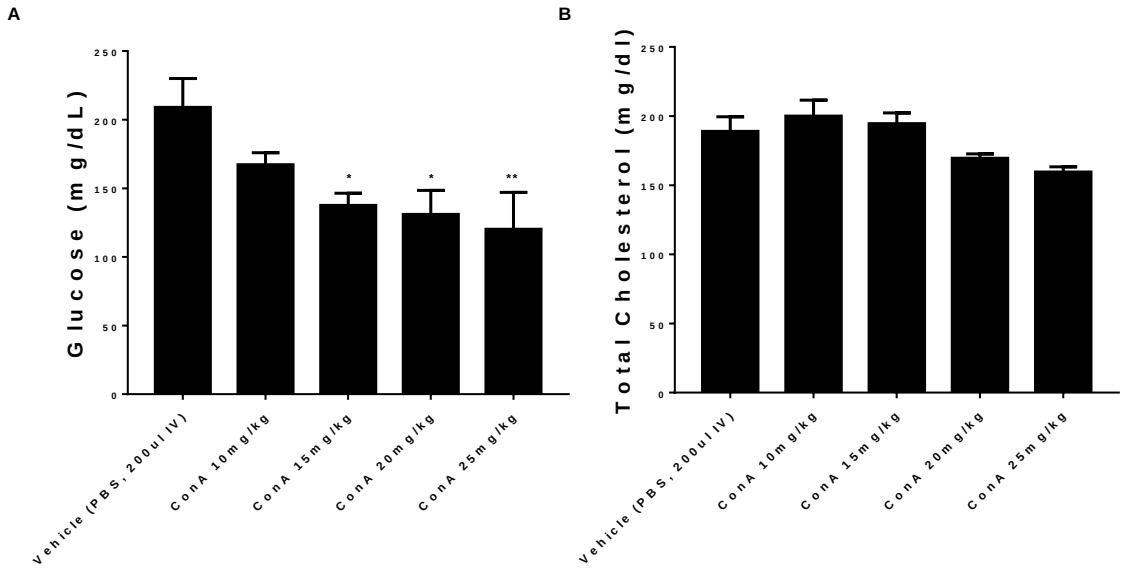

Figure 3-3 Response of glucose and cholesterol to intravenous concanavalin A administration. Lean male Balb/c mice were administered a single dose of concanavalin A intravenously. Serum levels of glucose **(A)** and cholesterol **(B)** were measured from serum collected 12 hours post-dose. Data are expressed as mean ± S.E.M. (n=6 mice/group). Significance is indicated *$P \leq 0.05$, **$P \leq 0.01$, treated group versus vehicle control group (Dunnett's one-way ANOVA).

We demonstrated that in our hands, concanavalin A administered intravenously acts as a potent immune cell mitogen in the liver, and damages hepatocytes dose-dependently through lymphocyte and macrophage-mediated mechanisms as measured by relevant clinical markers of liver function. However, how systemic and tissue-specific activin A and B levels are affected following concanavalin A administration has not been well characterized. To date, only activin A has been shown to be slightly increased following chronic (6 week) weekly IV administration of low dosage of concanavalin A (8 mg/kg) [37], which according to our data would be considered a sub-optimal dose to elicit relevant increases in clinical parameters of liver injury. Additionally, it has been demonstrated that concanavalin A is not suitable for development of chronic liver injury or disease, as mice become immunologically tolerant against concanavalin A-induced

liver inflammation after successful initial resolution (within roughly 8 days) [47]. Therefore, we measured circulating levels of both activin A and B following acute concanavalin A administration to ascertain whether systemic activin production is modulated in this disease model. What we found was that 12 hours following administration, circulating activin A levels were increased (although not significantly) at 10, 15, and 20 mg/kg dosages of concanavalin A. However, to our surprise, activin B levels showed a massive significant increase at every dosage of concanavalin A administered.

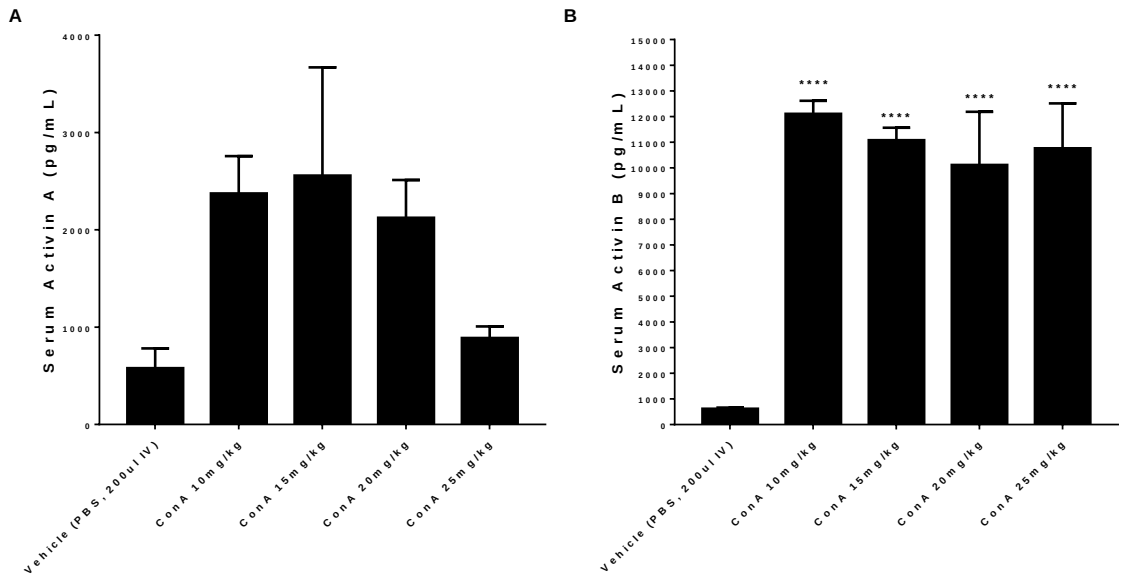

Figure 3-4 Systemic activin A and B levels following intravenous concanavalin A administration. Lean male Balb/c mice were administered a single dose of concanavalin A intravenously. Serum levels of activin A **(A)** and activin B **(B)** were measured by ELISA from serum collected 12 hours post-dose. Data are expressed as mean ± S.E.M. (n=6 mice/group). Significance is indicated ****$P \leq 0.0001$, treated group versus vehicle control group (Dunnett's one-way ANOVA).

Of particular interest regarding levels of activin B in circulation following concanavalin A administration is the fact that there is no correlation whatsoever to clinical parameters of liver

injury. Each dose of concanavalin A we evaluated saturated in terms of magnitude of increase in circulating activin B compared to control. Even at 10 mg/kg, where we saw no obvious increases to any markers of liver injury, increase in circulating activin B is equivalent to that seen in the 25 mg/kg group, where liver damage (as reflected by ALT and AST levels) is very appreciable. It is quite apparent that modulation of activin B plays an important role in the pathophysiology of immune-mediated liver injury, as reflected by the robust increase in circulating activin B in our study; cellular sources of activin B have not definitively been identified, however. Following stimulation with lipopolysaccharide, immunolocalization of inhibin βB has been performed via immunohistochemistry in mouse livers, which suggests vascular endothelial cells and Kupffer cells as potential sources [45], although there may be other sources of activin B production as well. We examined expression levels of inhibin A and B in both liver and spleen in this model to further identify where transcription of these genes may be modulated following immune-mediated injury to the liver.

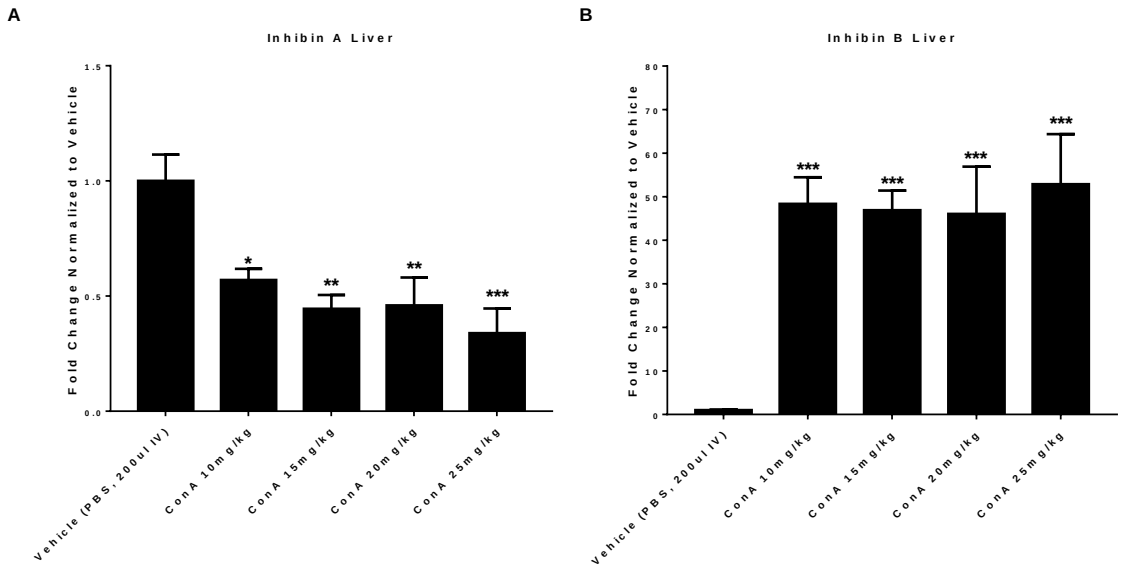

Figure 3-5 Inhibin A and B expression in the liver following intravenous concanavalin A administration. Lean male Balb/c mice were administered a single dose of concanavalin A intravenously. Transcript levels of inhibin A **(A)** and inhibin B **(B)** were quantified via qPCR using the $2^{-\Delta\Delta Ct}$ method from snap-frozen liver collected 12 hours post-dose, using hprt as the housekeeping gene. Data are expressed as mean ± S.E.M. (n=6 mice/group). Significance is indicated *P ≤ 0.05, **P ≤ 0.01, ***P ≤ 0.005, treated group versus vehicle control group (Dunnett's one-way ANOVA).

Following administration of concanavalin A, expression of inhibin A in the liver is significantly downregulated at 12 hours post dose for all dosages. In a model of acute inflammation induced by LPS administration, peak production of circulating activin A is achieved very quickly, within one hour of injection, and only remains slightly elevated compared to baseline from 3 hours up until 12 hours post administration [48]. This downregulation of activin A expression and only slight elevation in circulating ligand 12 hours post-dose may be in response to rapid, transient elevation of activin A following inflammatory response. In contrast, inhibin B transcription is highly upregulated (approximately 50-fold) 12 hours following concanavalin a administration, mimicking the massive increase seen in circulating ligand. It seems likely that due to the large

increase in expression of inhibin B, some population of resident liver cells or infiltrating immune cells are likely responsible for the increased production of circulating ligand.

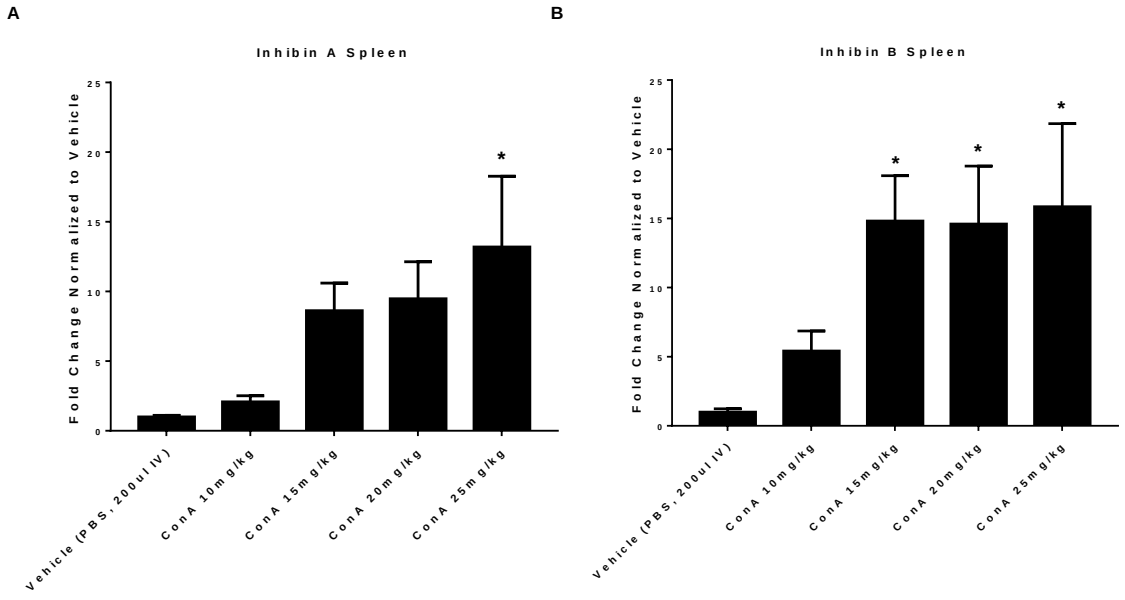

Figure 3-6 Inhibin A and B expression in the spleen following intravenous concanavalin A administration. Lean male Balb/c mice were administered a single dose of concanavalin A intravenously. Transcript levels of inhibin A **(A)** and inhibin B **(B)** were quantified via qPCR using the $2^{-\Delta\Delta Ct}$ method from snap-frozen spleen collected 12 hours post-dose, using beta-actin as the housekeeping gene. Data are expressed as mean ± S.E.M. (n=6 mice/group). Significance is indicated *$P \leq 0.05$, treated group versus vehicle control group (Dunnett's one-way ANOVA)

In the spleen, inhibin A expression is slightly upregulated starting at 15 mg/kg and dose-dependently increases, reaching significance at 25 mg/kg. This is not a surprising finding, given that stimulated CD4+ T-cells have been shown to produce activin A *in vitro* [33]. Regarding inhibin B, expression is increased to a larger extent than inhibin A, and is significantly increased from the 15 m/kg dosage on. This increase in transcription of inhibin B may be indicative of splenocytes an alternative source of activin B ligand in this model, be it activated T-cells, macrophages, or some other cell type. We also examined tissue-specific protein levels for

activin A and B in liver to corroborate whether increased expression led to increased local production of ligand.

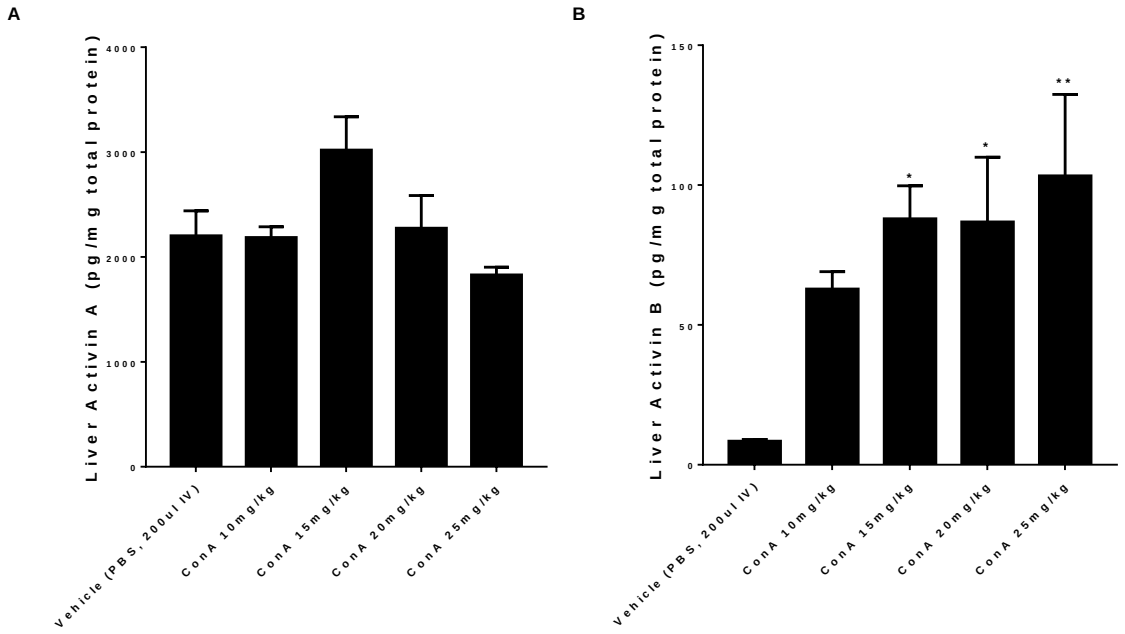

Figure 3-7 Liver activin A and B levels following intravenous concanavalin A administration. Lean male Balb/c mice were administered a single dose of concanavalin A intravenously. Tissue-specific levels of activin A **(A)** and activin B **(B)** were measured by ELISA from liver lysates collected 12 hours post-dose. Data are expressed as mean ± S.E.M. (n=6 mice/group). Significance is indicated *$P \leq 0.05$, **$P \leq 0.01$, treated group versus vehicle control group (Dunnett's one-way ANOVA).

In the liver, there are no significant changes to local production of activin A 12 hours following concanavalin A administration, consistent with serum levels and liver transcript data. Activin B production is dose-dependently increased in the liver following concanavalin A administration, reaching statistically significant difference at 15 mg/kg.

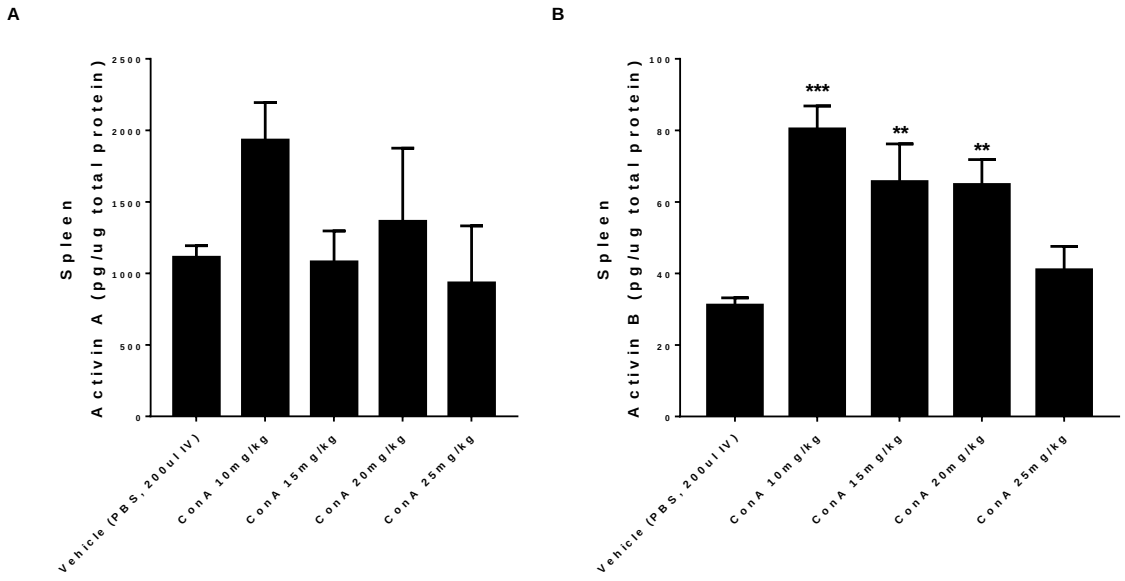

Figure 3-8 Spleen activin A and B levels following intravenous concanavalin A administration. Lean male Balb/c mice were administered a single dose of concanavalin A intravenously. Tissue-specific levels of activin A **(A)** and activin B **(B)** were measured by ELISA from spleen lysates collected 12 hours post-dose. Data are expressed as mean ± S.E.M. (n=6 mice/group). Significance is indicated **P ≤ 0.01, ***P ≤ 0.005, treated group versus vehicle control group (Dunnett's one-way ANOVA).

In the spleen, there are no significant changes to local production of activin A 12 hours following concanavalin A administration, even though we saw significant upregulation of inhibin A. Regarding activin B, there is a dose-dependent decrease in local ligand production, with the lowest dose of concanavalin A showing significant increase in ligand production and gradual reduction with increasing dose until reaching the highest dose, where activin B levels are similar to vehicle control. Following activation and clearance of antigen, activated T-cells need to be cleared in order to ensure tolerability in the periphery, maintain lymphocyte homeostasis and prevent autoimmunity [49]. Activation-induced cell death (AICD) is one mechanism though which apoptosis is induced in activated T-cells through re-stimulation of the T-cell receptor following initial activation and expansion [50]. It is likely in the higher dosage groups that re-stimulation of T-cells may be occurring during the contraction phase following initial stimulation, where activated T-cells are highly sensitive

to AICD [51], simply due to the fact that antigen may still be present and not fully cleared. This may explain why with increasing stimulation, we see decreasing protein production, as activated T-cells potentially responsible for production of activin B may be re-stimulated by concanavalin A not already cleared in the higher dosage groups, inducing cell death and leading to lower local production of ligand.

3.2 Antibody neutralization of activin A and B in concanavalin A immune-mediated hepatitis

We sufficiently characterized both activin A and B in response to acute liver injury induced by immune-mediated hepatitis though concanavalin A administration. We next sought to determine whether neutralization of either activin A or B might confer beneficial effects in this particular model. Animals were separated into five groups (n=8) and administered stimulation or treatments listed below (Table 3-2):

Table 3-2 Groups in concanavalin A activin A and B neutralization study

Group Number	Treatment	Stimulation
1	PBS (200 μL, SC)	PBS (200 μL, IV)
2	mIgG1 (50 mg/kg, SC)	ConA (15 mg/kg, IV)
3	Anti-Activin A (10 mg/kg, SC)	ConA (15 mg/kg, IV)
4	Anti-Activin B (50 mg/kg, SC)	ConA (15 mg/kg, IV)

Dosage of activin A antibody was determined from a previous study showing efficacy of muscular degeneration in a muscle injury model run previously [52]. Activin B antibody was shown to have an IC50 that was 5-fold higher than activin A antibody by Smad2/3 binding element promoter luciferase assay (data not shown), so we utilized a 5x dose compared to activin A antibody. We utilized a standard dose of 15 mg/kg for concanavalin A, as this was the lowest dosage to have

any sort of significant impact on clinical parameters of liver function, giving us the best chance to see effect following antibody treatment. Antibodies were dosed 16 hours prior to concanavalin A administration, and animals were sacrificed 12 hours following concanavalin A administration.

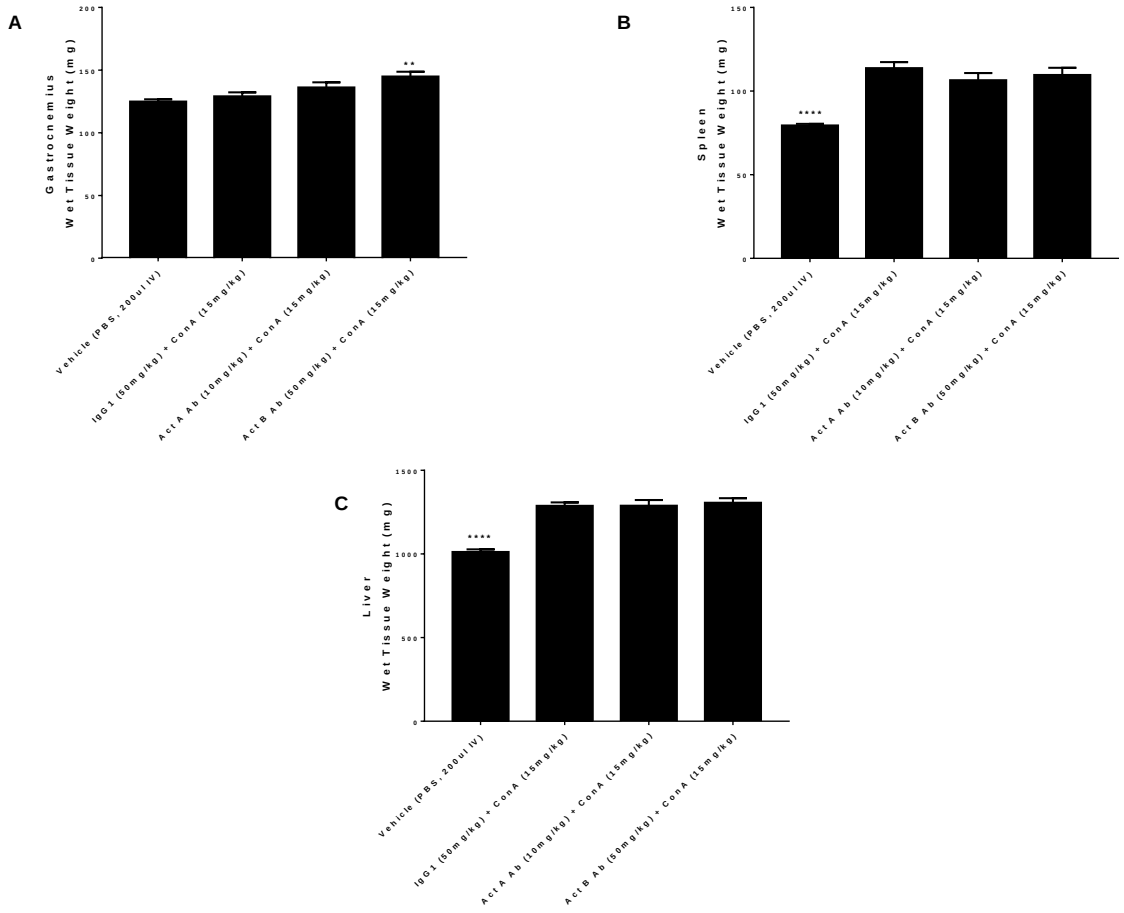

Figure 3-9 Tissue wet weights following activin antibody treatment and intravenous concanavalin A administration. Lean male Balb/c mice were administered antibody treatment listed and a single dose of concanavalin A intravenously 16 hours later. Wet tissue weights of gastrocnemius **(A)**, spleen **(B)**, and liver **(C)** were measured 12 hours post-dose. Data are expressed as mean ± S.E.M. (n=8 mice/group). Significance is indicated **P ≤ 0.01, ****P ≤ 0.001, treated group versus IgG control group (Dunnett's one-way ANOVA).

Concanavalin A administration significantly induces hepatomegaly and splenomegaly 12 hours following administration; neither activin A nor B antibody treatment was effective in reducing liver or spleen weight following concanavalin A insult. Interestingly, although there is no significant effect on muscle wasting in this model, activin B antibody treatment significantly increased muscle mass after only approximately 28 hours.

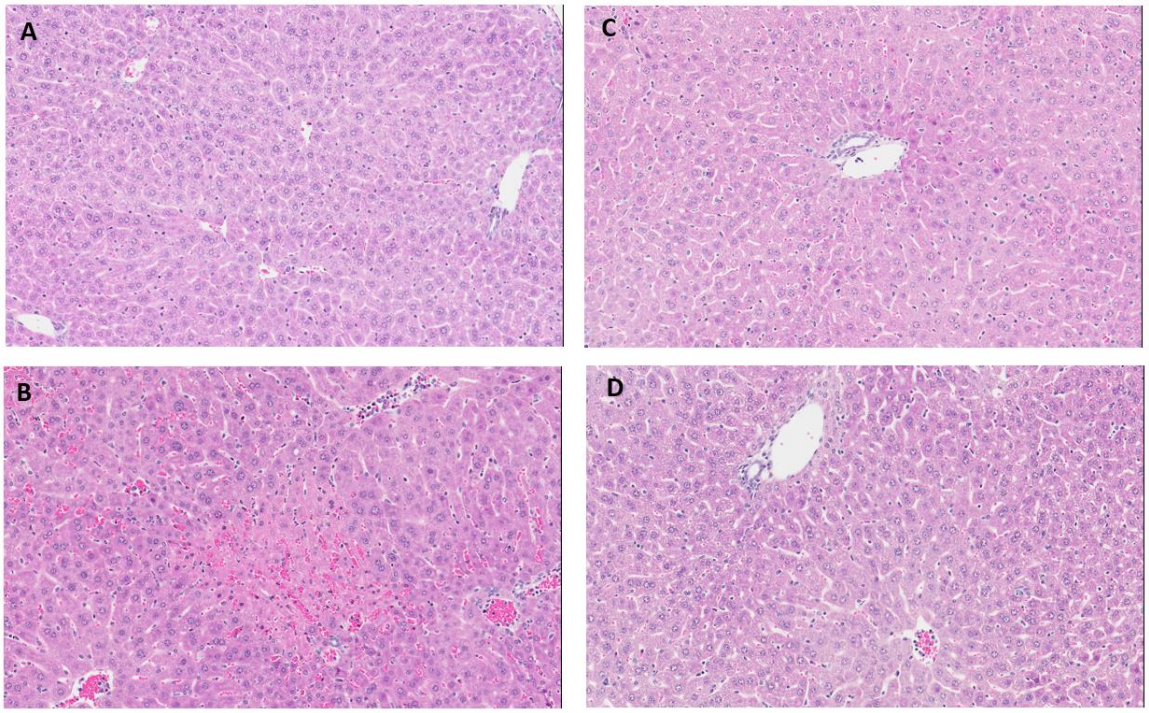

Figure 3-10 H&E staining in liver following activin antibody treatment and intravenous concanavalin A administration. Lean male Balb/c mice were administered antibody treatment listed and a single dose of concanavalin A intravenously 16 hours later. Liver sections were subjected to hematoxylin and eosin staining. Representative images of **(A)** PBS treated, **(B)** IgG + ConA, **(C)** anti-activin A + ConA, and **(D)** anti-activin B + ConA treatment are presented here.

Hematoxylin and eosin staining was performed on liver sections following study termination; concanavalin A treatment resulted in widespread necrotic damage to hepatocytes and cell death. In animals treated with either activin A or B antibody, this resulting damage to hepatocytes following concanavalin A administration was almost completely absent. This protective effect

on hepatocytes following inhibition of activin A or B is reflected by lowering of serum ALT and AST levels as well.

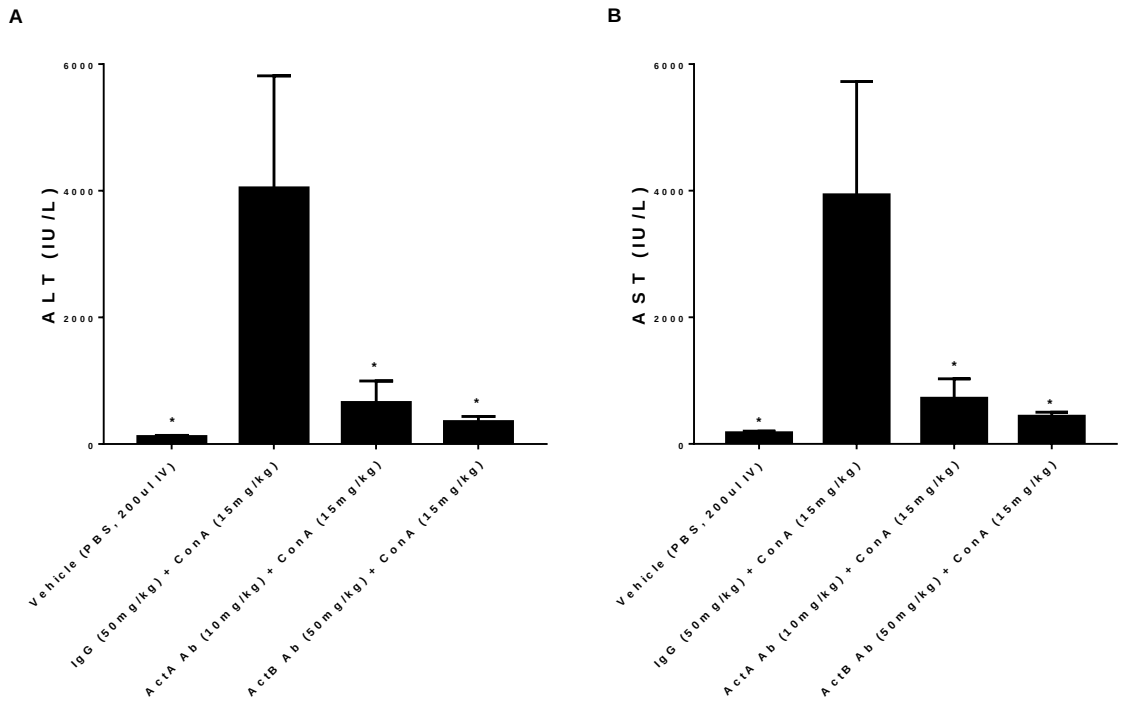

Figure 3-11 Response of ALT and AST following activin antibody treatment and intravenous concanavalin A administration. Lean male Balb/c mice were administered a single dose of antibody treatment listed and a single dose of concanavalin A intravenously 16 hours later. Serum levels of ALT **(A)** and AST **(B)** were measured from serum collected 12 hours post-dose. Data are expressed as mean ± S.E.M. (n=8 mice/group). Significance is indicated *$P \leq 0.05$, treated group versus IgG control group (Dunnett's one-way ANOVA).

Both activin A and B antibodies, when administered prophylactically prior to concanavalin A administration, showed significant reductions in ALT and AST in serum suggesting a protective effect of hepatocytes against injury induced by immune activation in the liver.

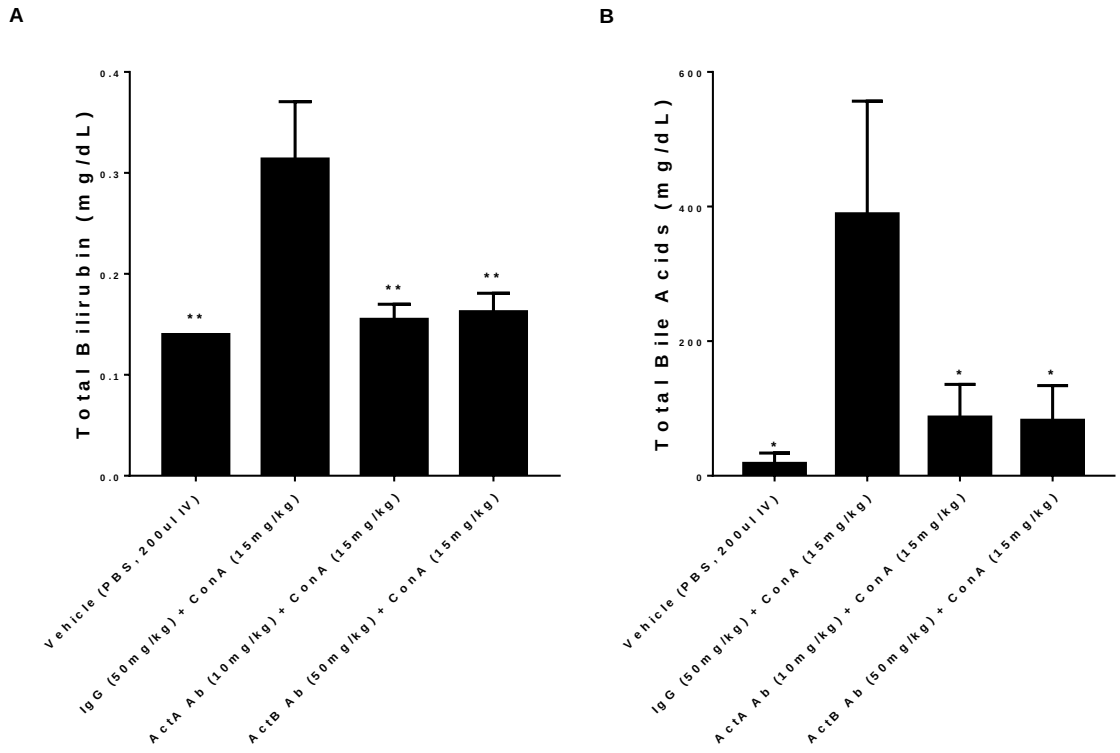

Figure 3-12 Response of bilirubin and bile acids following activin antibody treatment and intravenous concanavalin A administration. Lean male Balb/c mice were administered a single dose of antibody treatment listed and a single dose of concanavalin A intravenously 16 hours later. Serum levels of bilirubin **(A)** and bile acids **(B)** were measured from serum collected 12 hours post-dose. Data are expressed as mean ± S.E.M. (n=8 mice/group). Significance is indicated *P ≤ 0.05, **P ≤ 0.01 treated group versus IgG control group (Dunnett's one-way ANOVA).

Activin A and B antibodies also showed significant effects in lowering total bilirubin and reduction of total bile acids.

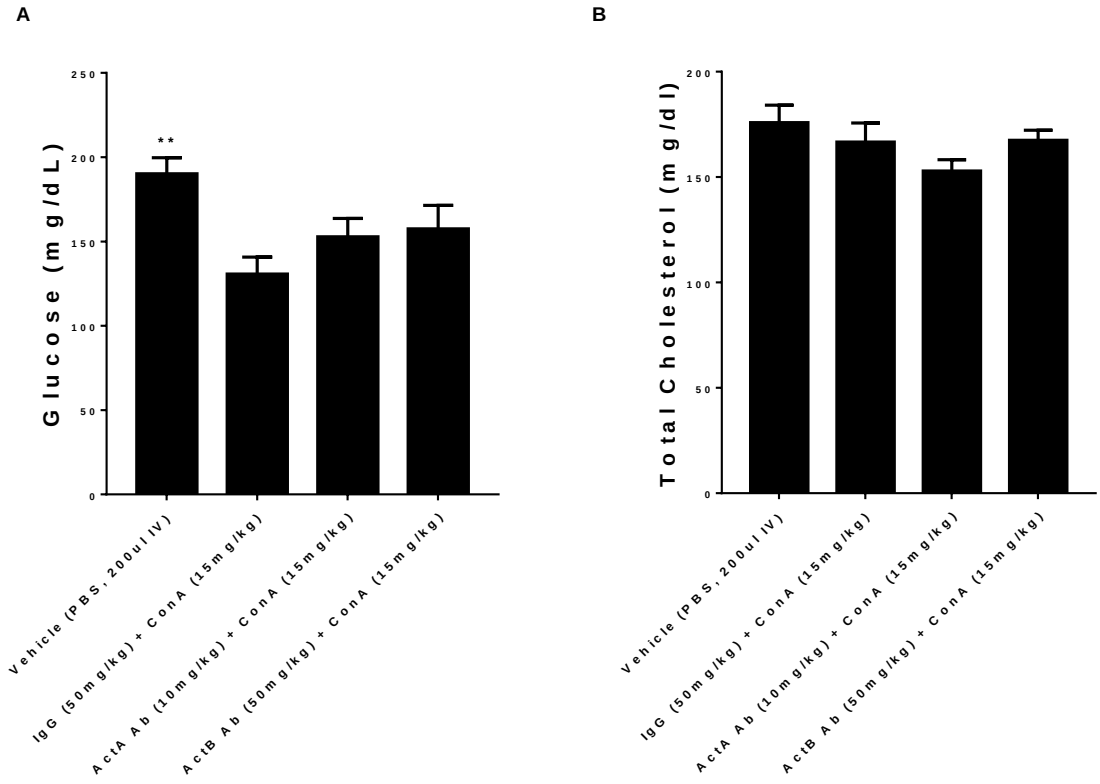

Figure 3-13 Response of glucose and cholesterol following activin antibody treatment and intravenous concanavalin A administration. Lean male Balb/c mice were administered a single dose of antibody treatment listed and a single dose of concanavalin A intravenously 16 hours later. Serum levels of glucose **(A)** and cholesterol **(B)** were measured from serum collected 12 hours post-dose. Data are expressed as mean ± S.E.M. (n=8 mice/group). Significance is indicated *P ≤ 0.05, **P ≤ 0.01 treated group versus IgG control group (Dunnett's one-way ANOVA).

Both antibody treatments showed a modest protection of gluconeogenesis (although not significant) following concanavalin A administration, and no effect on total cholesterol (although total cholesterol in this particular model does not seem to be affected).

Neutralization of both activin A and B conferred protective effects against immune-mediated liver injury induced by concanavalin A administration (reflected by significant reduction in serum ALT, AST, and bilirubin). To investigate mechanistically how neutralization of activin A

and B might confer these benefits, we analyzed IFN-γ, IL-1β, IL-2, IL-4, IL-5, IL-6, IL-10, IL-12p70, KC/GRO, and TNFα in terminal serum samples. Inhibition of activin A and B resulted in significant decreases in TNFα, IL-2, and IL-4.

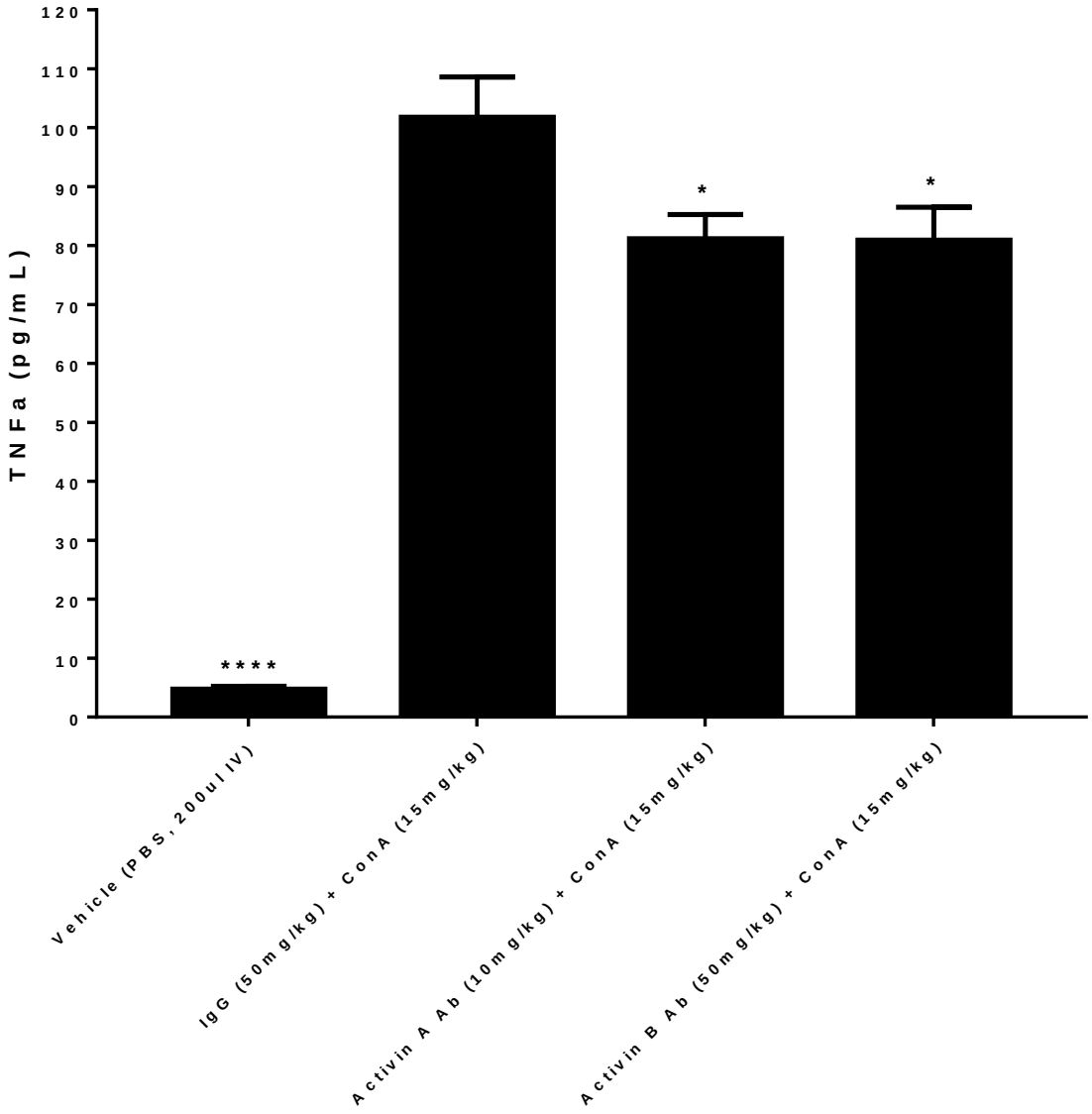

Figure 3-14 TNFα in serum following activin antibody treatment and intravenous concanavalin A administration. Lean male Balb/c mice were administered a single dose of antibody treatment listed and a single dose of concanavalin A intravenously 16 hours later. Serum levels of TNFα were measured via Meso Scale Discovery Electrochemiluminescence from serum collected 12 hours post-dose. Data are expressed as mean ± S.E.M. (n=8 mice/group). Significance is indicated *P ≤ 0.05, ****P ≤ 0.001 treated group versus IgG control group (Dunnett's one-way ANOVA).

Both activin A and B antibodies significantly reduced circulating levels of TNFα following concanavalin A administration. TNFα is a pleiotropic cytokine, produced by multiple immune

cell types including macrophages and monocytes and triggers multiple pathways involved in proliferation, inflammation, and apoptosis [53]. One major source of TNFα is phagocytosis of apoptotic hepatocytes by HSCs and Kupffer cells, leading to upregulation of TNFα and additional profibrogenic factors [54]. In regards to fibrosis, TNFα has been shown to induce proinflammatory and immunogenic activity in dendritic cell in the liver [55], and blocking TNFα has been shown to inhibit HSC activation by C-C motif chemokine receptor (CCR) 9+ macrophages [56]. It stands to reason that TNFα is an essential factor in the initialization and progression of liver fibrosis. Inhibition of activins in this case may reduce circulating levels of TNFα by prevention of hepatocyte death (as measured by ALT and AST), preventing TNFα production by HSCs and Kupffer cells engulfing apoptotic hepatocytes. How exactly activins may be involved in hepatocyte preservation in this disease model needs to further investigated.

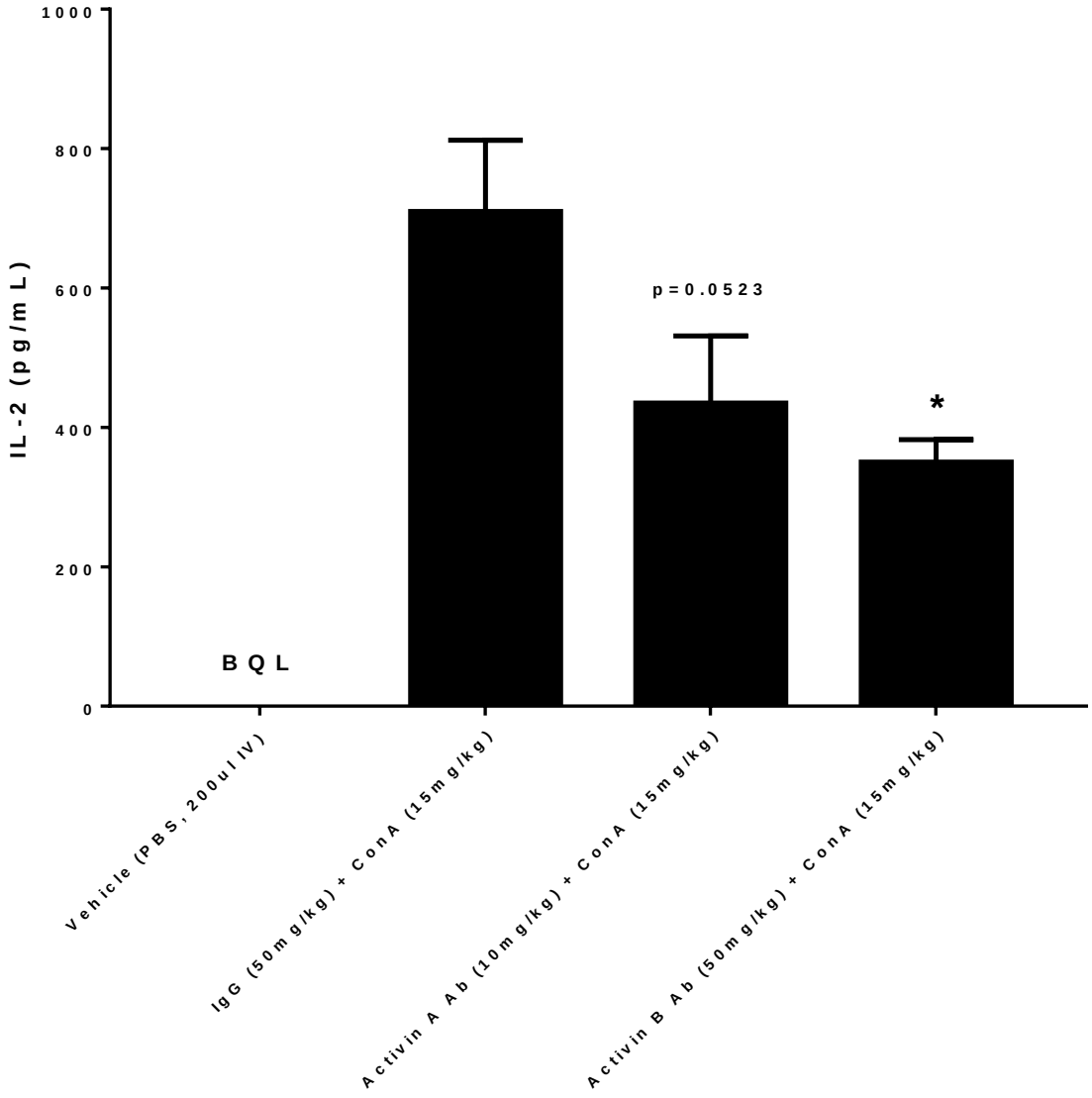

Figure 3-15 IL-2 in serum following activin antibody treatment and intravenous concanavalin A administration. Lean male Balb/c mice were administered a single dose of antibody treatment listed and a single dose of concanavalin A intravenously 16 hours later. Serum levels of IL-2 were measured via Meso Scale Discovery Electrochemiluminescence from serum collected 12 hours post-dose. Data are expressed as mean ± S.E.M. (n=8 mice/group). Significance is indicated *$P \leq 0.05$, treated group versus IgG control group (Dunnett's one-way ANOVA). BQL - below quantifiable limit.

Neutralization of activin B showed significant reduction of circulating IL-2, and neutralization of activin A reduced IL-2 to a lesser effect. IL-2 is primarily derived from activated $CD4^+$ T cells,

activated $CD8^+$ T cells, NK cells, dendritic cells and macrophages [57]. IL-2 plays a number of roles in immune regulation, many of which have implications regarding chronic injury and fibrosis, including: promoting T-cell differentiation to effector or memory cells when the T-cell is stimulated by antigen [57], development of proliferation-competent memory cells, priming of CD8+ cells with non-infectious immunogens, and maintenance of T-cells during chronic infection [58]. Reduction of IL-2 in this model is likely due to suppression of activation of T-cells and macrophages from concanavalin A stimulation.

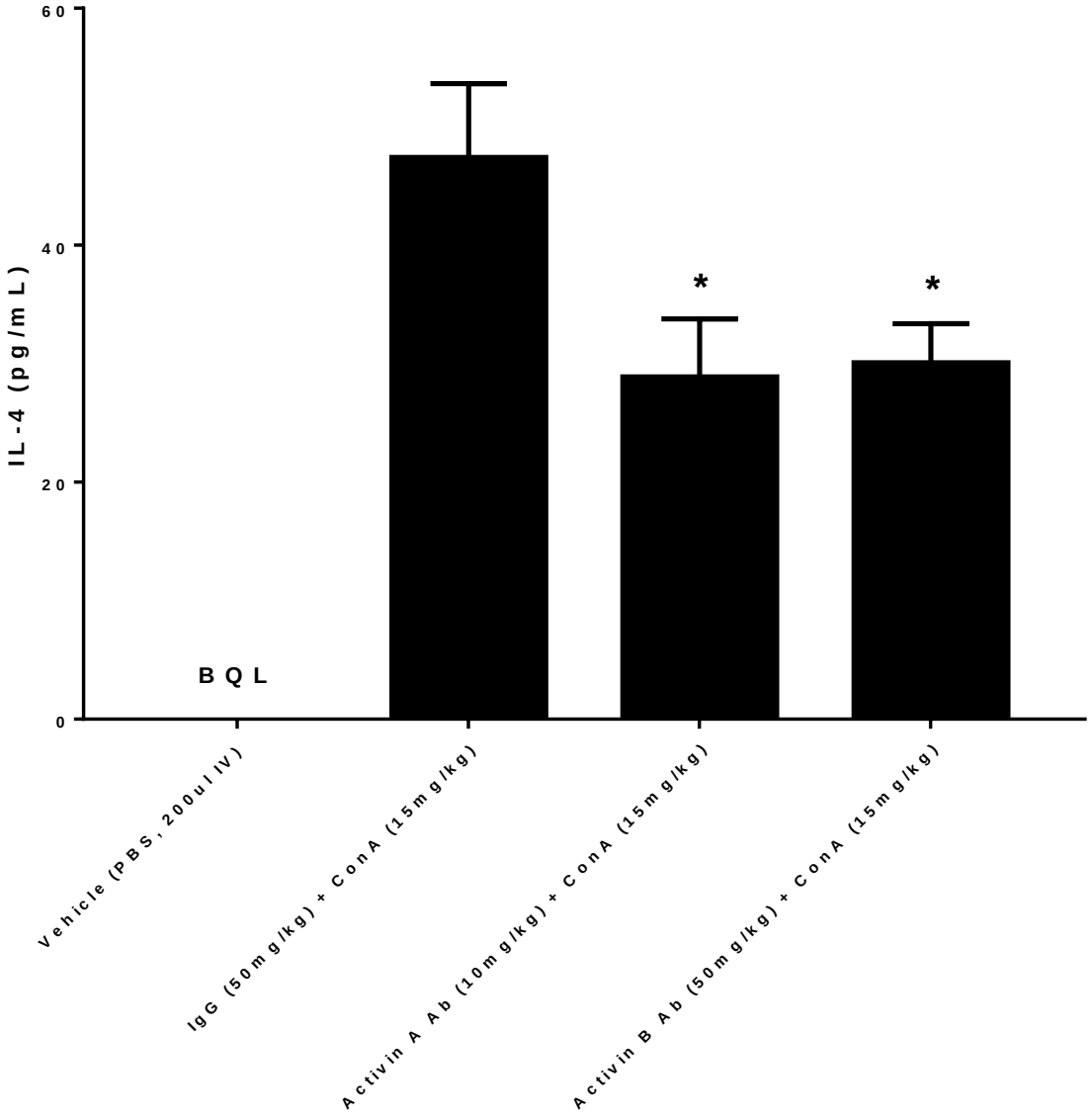

Figure 3-16 IL-4 in serum following activin antibody treatment and intravenous concanavalin A administration. Lean male Balb/c mice were administered a single dose of antibody treatment listed and a single dose of concanavalin A intravenously 16 hours later. Serum levels of IL-4 were measured via Meso Scale Discovery Electrochemiluminescence from serum collected 12 hours post-dose. Data are expressed as mean ± S.E.M. (n=8 mice/group). Significance is indicated *P ≤ 0.05, treated group versus IgG control group (Dunnett's one-way ANOVA). BQL - below quantifiable limit.

Both activin A and B neutralization resulted in significant lowering of IL-4 in circulation. IL-4 promotes alternative activation of resident macrophages in the liver into M2 macrophages, and

depending on context, M2 macrophages may exhibit pro or anti-fibrotic activity [59]. *In vivo*, IL-4/IL-13 double knockout animals (both of which bind IL-4Rα) showed resistance to development of fibrosis induced by CCL_4 administration, but deletion of IL-4Rα spontaneous fibrosis reversal is inhibited [59]. In this context, it is more likely that inhibition of IL-4 would be desirable to prevent development of fibrosis.

3.3 Antibody neutralization of activin A and B in CCl_4-induced liver fibrosis

We demonstrated that neutralization of activin A and B showed protective effects in an acute model of immune-mediated liver injury and showed potential for anti-fibrotic activity. We next sought to determine whether neutralization of activins could have the potential to reverse established fibrosis in a CCL_4-induced model of liver fibrosis. Mice were randomized by body weight (n=8) and administered corn oil or CCL_4. CCL_4 was injected twice weekly for 10 weeks; on the seventh week after the establishment of fibrosis, we began weekly administration of the following treatments:

Table 3-3 Groups in CCl_4 activin A and B neutralization study

Group Number	Treatment	Stimulation
1	PBS (10 mL/kg, SC)	Corn oil (10 mL/kg, IP)
2	mIgG1 (60 mg/kg, SC)	CCl_4 (1 mL/kg, IP)
3	Anti-Activin A (10 mg/kg, SC)	CCl_4 (1 mL/kg, IP)
4	Anti-Activin B (50 mg/kg, SC)	CCl_4 (1 mL/kg, IP)
5	Anti-A (10 mg/kg, SC) + Anti-B (50 mg/kg, SC)	CCl_4 (1 mL/kg, IP)
6	AcvRIIB Fc (10 mg/kg, SC)	CCl_4 (1 mL/kg, IP)

In this study, we included two extra groups: combination treatment of both activin A and B antibody, and pan inhibitor soluble decoy receptor AcvRIIB as a positive control. The combination group was included to test if neutralization of both ligands may have additive or synergistic effects in a fibrosis model.

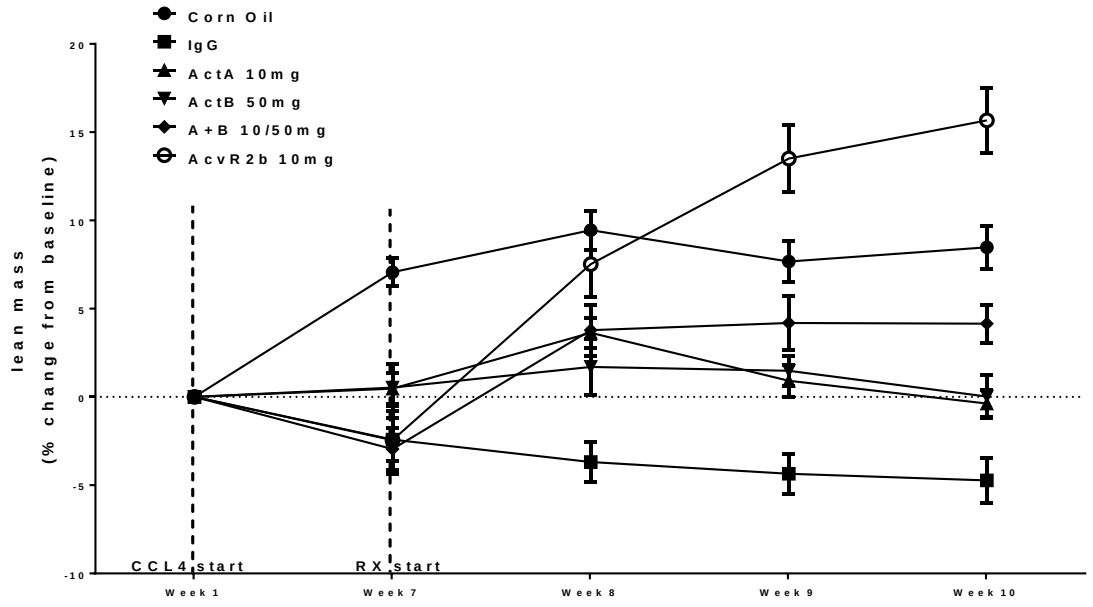

Figure 3-17 Lean mass % change from baseline following activin antibody treatment in CCl_4-induced hepatic fibrosis. Lean female C57bl/6 mice were administered weekly treatment listed after establishment of fibrosis. Weekly body composition was evaluated via qNMR, and lean mass reported as percent change from study baseline. Data are expressed as mean ± S.E.M. (n=8 mice/group).

Throughout the course of the study, body composition was monitored via qNMR. Muscle wasting is a common comorbidity associated with clinical hepatic fibrosis and end-stage liver disease, and incidence has been shown to progress with disease [60]. In our study, neutralization of activin A and B both had protective benefits to maintaining lean mass during progression of the disease. Combination treatment with both neutralizing antibodies had an enhanced effect and actually increased lean mass compared to baseline, suggesting neutralization of activin A and B

may confer this preservation of lean mass through different mechanisms or may modulate the activity of one another.

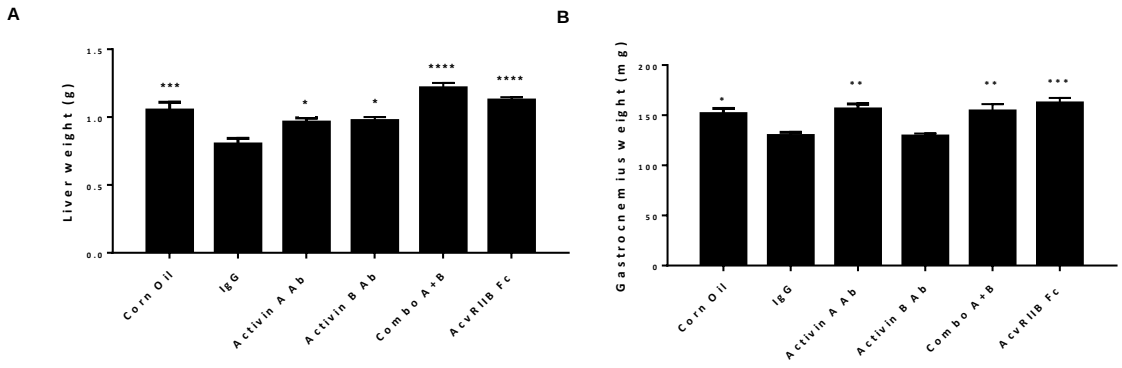

Figure 3-18 Tissue wet weights following activin antibody treatment in CCl_4-induced hepatic fibrosis. Lean female C57bl/6 mice were administered weekly treatment listed after establishment of fibrosis. Wet tissue weights of gastrocnemius **(A)** and liver **(B)** were measured at study termination. Data are expressed as mean ± S.E.M. (n=8 mice/group). Significance is indicated *P ≤ 0.05, **P ≤ 0.01, ***P ≤ 0.005, ****P ≤ 0.001, treated group versus IgG control group (Dunnett's one-way ANOVA).

At study termination, wet tissue weights of liver and gastrocnemius were taken. Neutralization of both activin A and B had the same magnitude of effect in maintaining liver weight, and combination of neutralizing both had an additive effect. Neutralization of activin A, but not activin B, maintained gastrocnemius weight; both combo neutralization and soluble receptor treatments had similar effect to activin A neutralization alone.

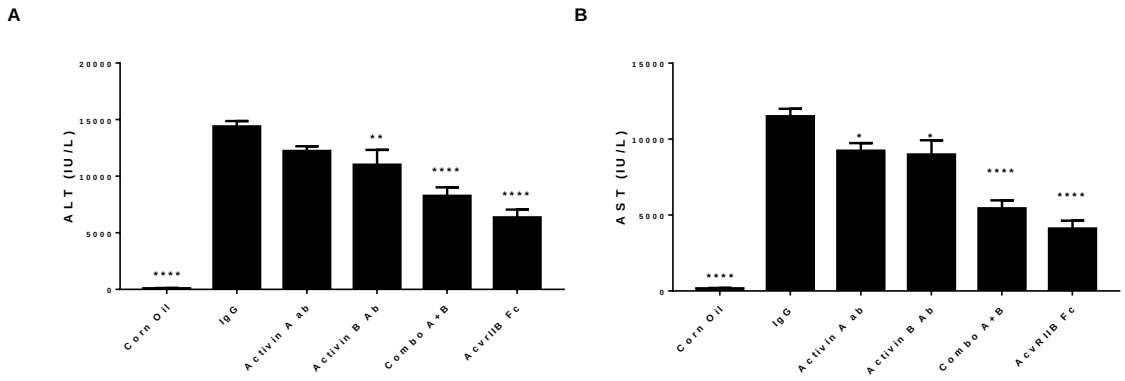

Figure 3-19 ALT and AST following activin antibody treatment in CCl_4-induced hepatic fibrosis. Lean female C57bl/6 mice were administered weekly treatment listed after establishment of fibrosis. Serum levels of ALT **(A)** and AST **(B)** were measured from serum collected at study termination. Data are expressed as mean ± S.E.M. (n=8 mice/group). Significance is indicated *P ≤ 0.05, **P ≤ 0.01, ***P ≤ 0.005, ****P ≤ 0.001, treated group versus IgG control group (Dunnett's one-way ANOVA).

Both activin A and B neutralization showed benefits in reducing serum ALT and AST after establishment of fibrosis, and the severity of the liver injury at this point is quite apparent due to the massive increase in ALT and AST in circulation compared to corn oil treated controls. Additionally, neutralization of both activins resulted in a marked decrease in both ALT and AST compared to either treatment alone.

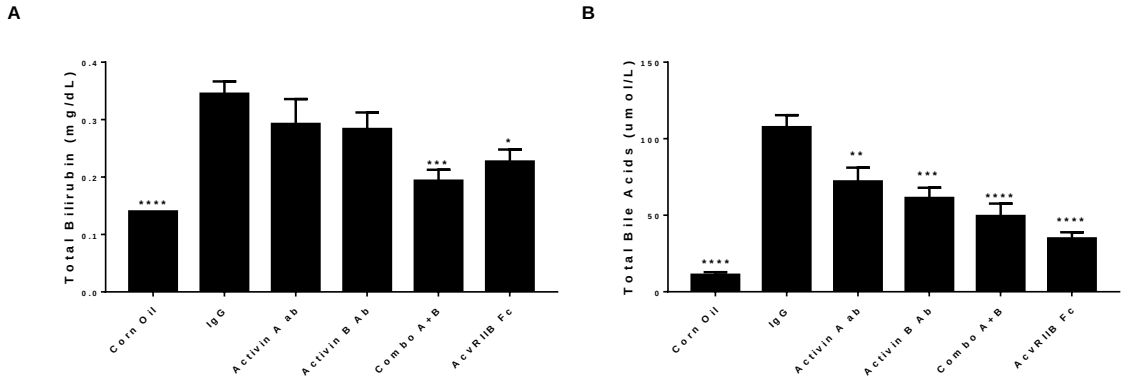

Figure 3-20 Bilirubin and bile acids following activin antibody treatment in CCl_4-induced hepatic fibrosis. Lean female C57bl/6 mice were administered weekly treatment listed after establishment of fibrosis. Serum levels of bilirubin **(A)** and bile acids **(B)** were measured from serum collected at study termination. Data are expressed as mean ± S.E.M. (n=8 mice/group). Significance is indicated *P ≤ 0.05, **P ≤ 0.01, ***P ≤ 0.005, ****P ≤ 0.001, treated group versus IgG control group (Dunnett's one-way ANOVA).

Neither neutralization of activin A nor B alone significantly reduced bilirubin, but when neutralized in combination a significant lowering was seen compared to control. Neutralization of A and B separately (B more so than A) significantly lowered bile acids. Neutralization of both ligands slightly improved this reduction.

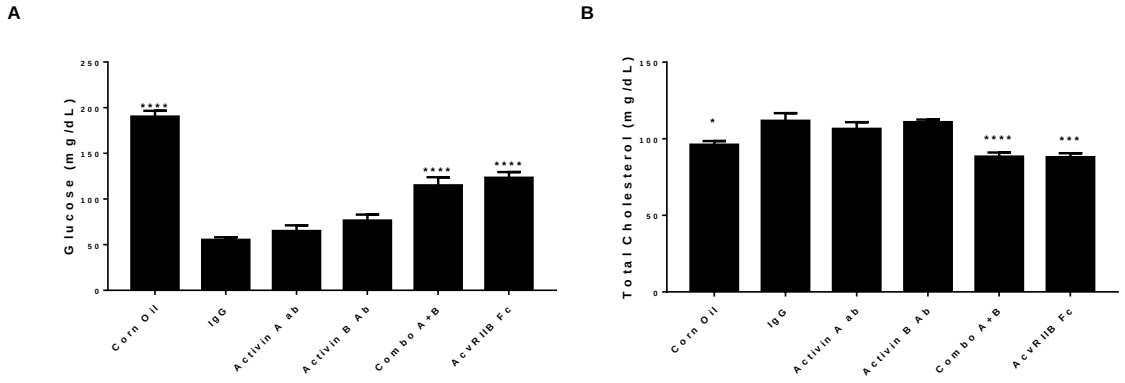

Figure 3-21 Glucose and cholesterol following activin antibody treatment in CCl_4-induced hepatic fibrosis. Lean female C57bl/6 mice were administered weekly treatment listed after establishment of fibrosis. Serum levels of glucose **(A)** and cholesterol **(B)** were measured from serum collected at study termination. Data are expressed as mean ± S.E.M. (n=8 mice/group). Significance is indicated *P ≤ 0.05, ***P ≤ 0.005, ****P ≤ 0.001, treated group versus IgG control group (Dunnett's one-way ANOVA).

Glucose levels were not significantly improved by neutralization of either activin A or B alone, but combination neutralization of both ligands resulted in a highly significant improvement. Likewise, neutralizing either ligand alone showed no improvement in cholesterol in serum, but combination neutralization significantly reduced cholesterol to levels below corn oil control.

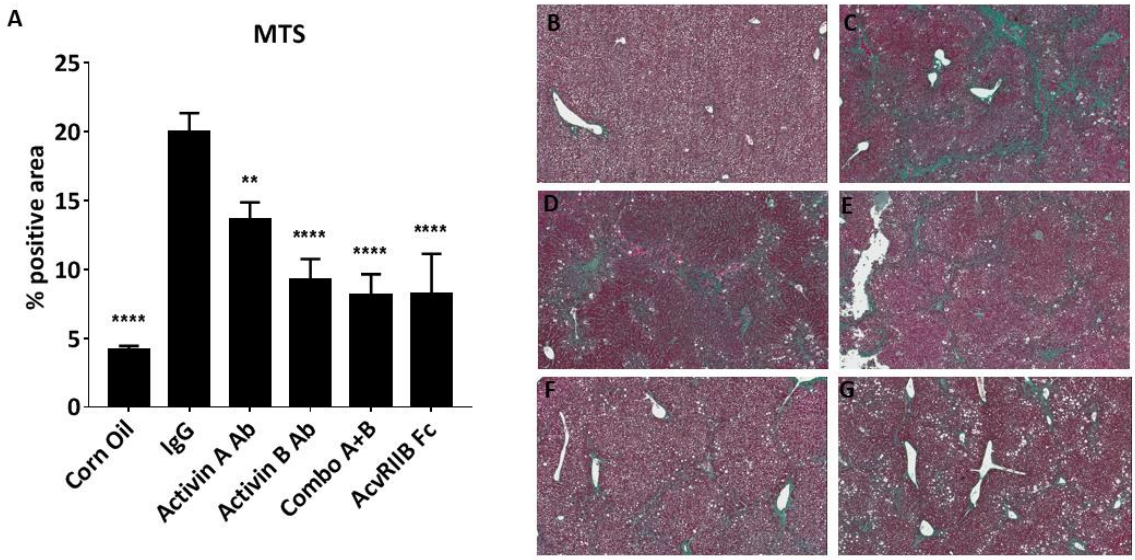

Figure 3-22 MTS staining in liver following activin antibody treatment in CCl_4-induced hepatic fibrosis. Lean female C57bl/6 mice were administered weekly treatment listed after establishment of fibrosis. Liver sections were subjected to Masson's trichrome staining and **(A)** % positive area staining for collagen was quantified using ImageJ. Representative images of **(B)** corn oil, **(C)** IgG, **(D)** anti-activin A, **(E)** anti-activin B, **(F)** antibody combination, and **(G)** AcvRIIB Fc treatment are presented here. Data are expressed as mean ± S.E.M. (n=8 mice/group). Significance is indicated **P ≤ 0.01, ****P ≤ 0.001, treated group versus IgG control group (Dunnett's one-way ANOVA).

A main endpoint of this study was to perform Masson's trichrome staining on liver sections in order to visualize and quantitate collagen deposition and fibrosis following CCl_4 administration and demonstrate if inhibition of either activin may reverse disease progression. The results from 10 weeks of CCl_4 administration are quite striking – nearly 20% of the liver of IgG treated animals is fibrotic. This fibrosis is prevalent throughout the entire liver, and is not contained to only areas surrounding vasculature. Even more surprising is the marked effect neutralization of activin A and B has in reducing fibrosis in this model. Both A, and to greater effect B, significantly reduce fibrosis; there does not seem to be increased effect when both ligands are neutralized.

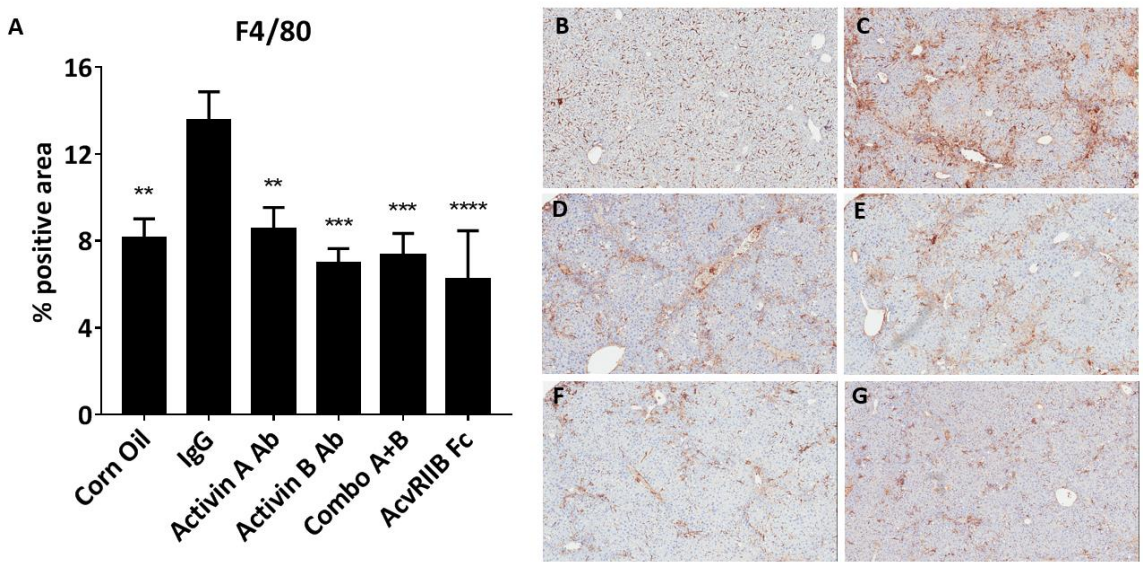

Figure 3-23 F4/80 staining in liver following activin antibody treatment in CCl_4-induced hepatic fibrosis. Lean female C57bl/6 mice were administered weekly treatment listed after establishment of fibrosis. Liver sections were stained with anti-F4/80 and **(A)** % positive area staining was quantified using ImageJ. Representative images of **(B)** corn oil, **(C)** IgG, **(D)** anti-activin A, **(E)** anti-activin B, **(F)** antibody combination, and **(G)** AcvRIIB Fc treatment are presented here. Data are expressed as mean ± S.E.M. (n=8 mice/group). Significance is indicated **$P \leq 0.01$, ***$P \leq 0.005$, ****$P \leq 0.001$, treated group versus IgG control group (Dunnett's one-way ANOVA).

Immunostaining of liver sections with anti-F4/80 was also performed and quantitated - F4/80 is a marker of murine macrophages and Kupffer cells. CCl_4 administration significantly increased macrophage infiltration into the liver compared to corn oil treated mice. Neutralization of activin A, B, and the combination all were effective in significantly reducing macrophage numbers to near baseline levels. There did not seem to be any sort of additive or synergistic effects in combination neutralization of both ligands.

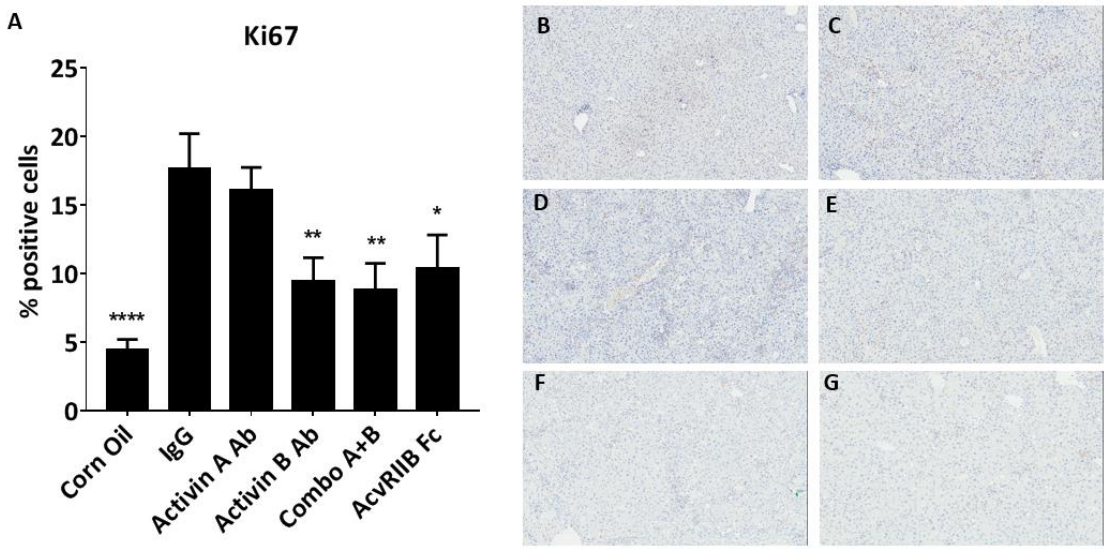

Figure 3-24 Ki67 staining in liver following activin antibody treatment in CCl_4-induced hepatic fibrosis. Lean female C57bl/6 mice were administered weekly treatment listed after establishment of fibrosis. Liver sections were stained with anti-Ki67 and **(A)** % positive cells stained was quantified using ImageJ. Representative images of **(B)** corn oil, **(C)** IgG, **(D)** anti-activin A, **(E)** anti-activin B, **(F)** antibody combination, and **(G)** AcvRIIB Fc treatment are presented here. Data are expressed as mean ± S.E.M. (n=8 mice/group). Significance is indicated *$P \leq 0.05$, **$P \leq 0.01$, ****$P \leq 0.001$, treated group versus IgG control group (Dunnett's one-way ANOVA).

Proliferative action in the liver was quantified by Ki67 staining. In the context of liver, increase in proliferation is largely reflective hepatocytes re-entering the cell cycle from quiescence following damage [61]. This increase in proliferation may also be reflective of the activation of HSCs into proliferative, pro-fibrogenic myofibroblast-like cells. CCl_4 administration resulted in significant positive staining of Ki67 compared to corn oil treatment, suggesting widespread damage and apoptosis in hepatocytes and activation of HSCs. Neutralization of activin B, but not activin A, significantly reduced this proliferation seen with CCl_4 administration; neutralization of both antibodies in combination did not improve effect compared to B neutralization alone.

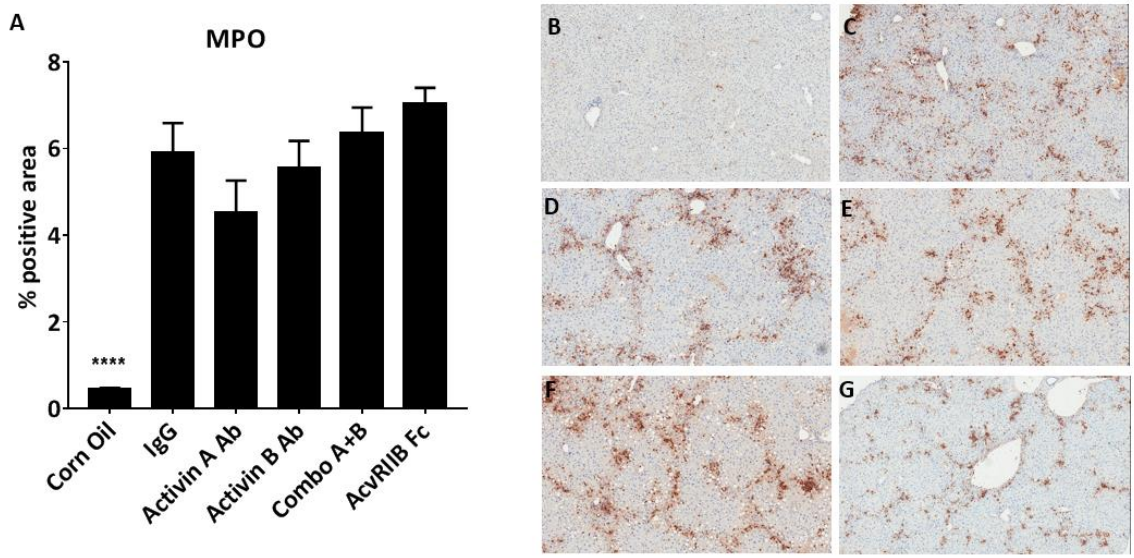

Figure 3-25 MPO staining in liver following activin antibody treatment in CCl_4-induced hepatic fibrosis. Lean female C57bl/6 mice were administered weekly treatment listed after establishment of fibrosis. Liver sections were stained with anti-MPO and **(A)** % positive area staining was quantified using ImageJ. Representative images of **(B)** corn oil, **(C)** IgG, **(D)** anti-activin A, **(E)** anti-activin B, **(F)** antibody combination, and **(G)** AcvRIIB Fc treatment are presented here. Data are expressed as mean ± S.E.M. (n=8 mice/group). Significance is indicated *$P \leq 0.05$, **$P \leq 0.01$, ****$P \leq 0.001$, treated group versus IgG control group (Dunnett's one-way ANOVA).

Myeloperoxidase (MPO) is a peroxidase enzyme abundantly expressed in neutrophil granulocytes – in normal and acutely damaged rat liver, MPO expression is only found in neutrophil granulocytes, but not in macrophages [62]. CCl_4 administration significantly increased neutrophil infiltration into liver compared to corn oil treated animals, but neither activin A, activin B, or the neutralization of both showed any effects on neutrophils in the liver.

Neutralization of activin A and B individually both showed significant improvements in parameters of liver damage, liver function, fibrosis, and macrophage infiltration in a CCl_4-induced model of liver fibrosis after establishment of disease. Activin B neutralization showed a

more robust effect in reducing fibrosis and also significantly reduced hepatocyte and HSC proliferation which activin A neutralization did not. Combination neutralization of both ligands showed additive or synergistic effects in certain parameters, including protection of hepatocytes (via reduced ALT and AST), gluconeogenesis, cholesterol metabolism, bilirubin and bile acid production, and preservation of lean mass. Overall, neutralization of activin A, B, and the combination of both showed profound benefits in this experimental model of liver fibrosis.

CHAPTER 4. DISCUSSION

4.1 Characterization of concanavalin A induced immune hepatitis

Tissue injury and the resulting inflammatory response acts as an important trigger for the initiation of regenerative processes and the development of fibrosis; in many diseases this inflammatory response is essential for fibrosis to occur at all [63]. Understanding how activins are modulated during this initial inflammatory response may provide insights as to if and how they may affect the initiation and progression of liver fibrosis. Concanavalin A-induced hepatitis provides a convenient, short-term model of inflammation highly specific to the liver mediated through activation of T-cells and macrophages. Concanavalin A may also have direct stimulatory effects on resident HSCs, a major cellular contributor to the initiation and progression of fibrosis. HSCs directly stimulated by concanavalin A have been shown to induce oxidative stress and apoptosis of hepatocytes in the absence of other effector cell types [64]. In our hands, concanavalin A administration resulted in trademarks of severe, acute inflammatory response in the liver – increases in enzymes reflective of hepatocyte death (ALT and AST), and impaired function (serum bilirubin and glucose). We demonstrated how activins are modulated during this acute phase inflammation – circulating activin B levels were massively increased, nearly 20 fold compared to control animals. It is clear that activin B production is to a certain extent hepatically derived, as reflected by a roughly 50-fold increase in inhibin B expression and significant increase in liver-specific protein. However, this substantial increase in circulating activin B was even observed in dosages of concanavalin A where there were no measureable effects on clinical parameters of liver injury or function. This finding is suggestive of some subpopulation of activated immune cells potentially being an alternative source of activin B

production during the inflammatory phase. To further support this notion we also observed significant increases in inhibin B expression and activin B protein in the spleen. Measurement of activin B by ELISA in the conditioned cell media of stimulated splenocytes would be a simple method of ascertaining whether or not some leukeocyte may be responsible for production of activin B. Regarding activin A, we saw only slight effects in circulating protein 12 hours following stimulation of concanavalin A. As previously mentioned, in a model of LPS-induced liver inflammation, activin A production was significantly increased immediately following stimulation, but dropped rapidly 3 hours following stimulation [48]. In the content of the concanavalin A model, is very likely that production of activin A by inflammatory insult is very rapid and transient, and 12 hours following initial stimulation levels have already decreased substantially. This notion is further supported by the fact that we observe significant downregulation of activin A in the liver at 12 hours post-stimulation, likely due to inhibitory feedback from initial signaling. Ideally, it would be best to perform characterization of this model throughout the entire time course of stimulation, from the initial inflammatory response all the way to resolution. Regardless, our characterization of this model demonstrated the modulation of activins in the context of acute liver inflammation, and therefore how activins might be involved in the pathology of fibrosis.

4.2 Antibody neutralization of activin A and B in concanavalin A-induced immune hepatitis

Neutralization of activin A and B conferred pronounced effects in our concanavalin A immune-mediated hepatitis model – blocking either A or B protected hepatocytes and significantly lowered ALT and AST in the serum at 12 hours post-stimulation, and improved liver function (significantly decreased serum bilirubin). We saw significant reductions in serum cytokines

TNFα, IL-2, and IL-4 when neutralizing activin A or B prior to concanavalin A stimulation. TNFα is a known promoter of liver fibrosis; inflammation in the liver is perpetuated by TNFα production, which results in the activation of resident HSCs into fibrogenic myofibroblasts [53]. TNFα has also been shown to directly induce apoptosis in hepatocytes [65]. Mechanistically, it is uncertain how exactly activin neutralization is modulating TNFα in this model. Phagocytosis of apoptotic hepatocytes by HSCs or macrophages upregulates TNFα, and chronic activation of these cells accelerates hepatocyte apoptosis and inflammation, leading to a positive feedback loop [54]. Activin neutralization may inhibit activation or recruitment of macrophages during acute inflammation, blunting the upregulation of TNFα from phagocytosis of apoptotic hepatocytes. Activin neutralization may also inhibit the activity of concanavalin A to stimulate activation of HSCs. Examining histological markers of macrophages and proliferation might provide clues as to how exactly activin neutralization downregulates TNFα. IL-2 is a Th1 cytokine, responsible for macrophage activation among other functions [66]. This downregulation of IL-2 may provide an explanation as for the downregulation of TNFα we observed, as macrophage activation may be inhibited. The main source of IL-2 in this model is likely from activated T-cells; activins may play a role in the activation or proliferation of T-cells following stimulation. It may be beneficial to explore this relationship by characterizing isolated CD3+ cells and subpopulations after treatment with exogenous activins. IL-4 is a Th2 cytokine, responsible for induction of naïve T-helper cells to Th2 cells – it also promotes alternative polarization of macrophages to M2 macrophages and inhibits M1 polarization. Acutely, M2 macrophages promote controlled wound healing and tissue regeneration though IL-10, TGFβ, and other secreted factors [67]. When chronically activated, however, M2 macrophages can activate resident fibroblasts and promote fibrosis [68]; downregulation of IL-4 in chronic liver injury may confer anti-fibrotic effects and

inhibit the progression of fibrogenesis. Overall, neutralization of activins confers benefits during acute-phase inflammation, and may confer benefits during chronic inflammation and fibrogenesis.

4.3 Antibody neutralization of activin A and B in carbon tetrachloride-induced liver fibrosis

We characterized activins in the context of the acute inflammatory phase, demonstrated protective effects in the liver via inhibition of activins following immune stimulation, and provided some insight mechanistically as to how activin inhibition may be conferring these benefits and how activin modulation may be involved in chronic inflammation and the initiation and progression of fibrosis. The final step was to characterize the effects of activin neutralization in an experimental model of liver fibrosis. CCl_4 is a commonly used, highly potent, and well-characterized hepatotoxin used in preclinical rodent models to induce liver fibrosis; CCl_4 increases lipid profile, liver enzymes, and oxidative stress markers, while decreasing total protein and high-density lipoprotein [69]. More importantly, histological changes in inflammation, loss of normal hepatocytes, collagen deposition and fiber segmentation formation are observed following CCl_4 administration [70]. This collagen deposition and ECM formation is driven by recruitment and activation of HSCs to the site of tissue injury, which transdifferentiate into myofibroblast-like cells, driven by increased TGFβ signaling [71]. In our experiment, we opted to allow for development of disease by administering CCl_4 without therapy for six weeks, to evaluate the effect of activin neutralization in a therapeutic modality versus preventative. We observed striking results following CCl_4 administration for 10 weeks: a massive increase in liver damage enzymes, marked decreases in parameters of liver function, severe impact on gluconeogenesis, profound infiltration of macrophages, proliferation of

hepatocytes and HSCs, pervasive collagen deposition, and collection and retention of ascetic fluid in the abdomen. CCl4 administration over a 10-week period is representative of clinical presentation of advanced liver disease with concurrent fibrosis. Regardless of the severity of the model, neutralization of activins showed drastic effects in resolving complications from inflammatory insult and fibrogenesis resulting from CCl_4 administration. We saw improvements in liver function, protection from liver damage, resolution of fibrosis, and reduction in macrophage infiltration. The reduction we see in chronic recruitment and activation of macrophages may be explained by the reduction of TNFα we saw during the acute inflammatory phase when inhibiting activins. Reduced circulating IL-2 and IL-4 we observed during acute inflammation following activin neutralization would reflect decreased polarization of macrophages towards M1 and M2 states during chronic injury, respectively, modulating the acute pro-inflammatory response (M1) throughout disease progression as well as fibrotic responses, ECM deposition, and fibroblast activation (M2). Additionally, we observed some differentiation between activin A and B neutralization in this model. Activin B inhibition resulted in a significant reduction in proliferation, and overall had better effects in resolving fibrosis than activin A inhibition. Mechanistically, activin B is involved in the activation and proliferation of HSCs and proliferation of hepatocytes following apoptosis either directly or indirectly (as indicated by significant effects on proliferation), which also explains the enhanced reduction in fibrosis versus activin A inhibition alone. It is worth exploring this distinction of activin B from A, by characterizing the stimulatory response of isolated hepatocytes or HSCs to exogenous activin A or B treatment. Finally, we observed some additive or synergistic effects when both activin A and B were neutralized in this model. Combination therapy improved protection of hepatocytes (via reduced ALT and AST), gluconeogenesis, cholesterol metabolism,

liver function, and preservation of lean mass; these improvements in combination therapy versus individual inhibition of either ligand alone suggests activin A and B may be operating through different pathways to confer similar effects, or that the two ligands may modulate the activities of one another. These observations warrant further investigation into the dynamics of actin A and B signaling in relation to one another, in particular regard to muscle metabolism which was unfortunately beyond the scope of the work performed here. Overall, neutralization of either or both ligands showed promising liver protective and anti-fibrotic activity in our pre-clinical model of liver fibrosis.

4.4 Conclusions

Tissue injury and the resulting acute inflammatory response is an essential stimuli for the initiation and progression of fibrosis encountered during chronic liver disease. Using an immune-mediated model of acute liver inflammation, we were able to characterize resulting liver damage and impairments to liver function following insult and how activin A and B are modulated during this initial response. We provided mechanistic insights into activin A and B activity in the context of acute inflammation by neutralization via antibody in our concanavalin A model, and demonstrated the protective effects of inhibition of these ligands. Finally, we showed how activin A and B neutralization inhibited liver injury, improved liver function, and reduced fibrosis in a chronic model of CCl_4-induced liver fibrosis and explored mechanistically how neutralizing activins conferred these benefits. Our data taken together suggest activin A and B as important players during not only initial inflammatory response, but also during chronic, sustained inflammation and fibrogenesis in the liver and show the therapeutic potential of targeting of these ligands in chronic liver disease and fibrosis.

REFERENCES

1. Friedman, S. L. Liver fibrosis -- from bench to bedside. *J. Hepatol.* **38 Suppl 1**, S38-53 (2003).

2. Sanyal, A. J. Novel therapeutic targets for steatohepatitis. *Clin. Res. Hepatol. Gastroenterol.* **39**, S46–S50 (2015).

3. Dechêne, A. *et al.* Acute liver failure is associated with elevated liver stiffness and hepatic stellate cell activation. *Hepatology* **52**, 1008–1016 (2010).

4. Pellicoro, A., Ramachandran, P., Iredale, J. P. & Fallowfield, J. A. Liver fibrosis and repair: immune regulation of wound healing in a solid organ. *Nat. Rev. Immunol.* **14**, 181–194 (2014).

5. Bataller, R. & Brenner, D. A. Liver fibrosis. *J. Clin. Invest.* **115**, 209–218 (2005).

6. LAROSA, D. & ORANGE, J. 1. Lymphocytes. *J. Allergy Clin. Immunol.* **121**, S364–S369 (2008).

7. Butcher, E. C. & Picker, L. J. Lymphocyte homing and homeostasis. *Science* **272**, 60–6 (1996).

8. Fazilleau, N., McHeyzer-Williams, L. J., Rosen, H. & McHeyzer-Williams, M. G. The function of follicular helper T cells is regulated by the strength of T cell antigen receptor binding. *Nat. Immunol.* **10**, 375–84 (2009).

9. Holt, A. P., Salmon, M., Buckley, C. D. & Adams, D. H. Immune interactions in hepatic fibrosis. *Clin. Liver Dis.* **12**, 861–82, x (2008).

10. Melhem, A. *et al.* Anti-fibrotic activity of NK cells in experimental liver injury through killing of activated HSC. *J. Hepatol.* **45**, 60–71 (2006).

11. Friedman, S. Cytokines and Fibrogenesis. *Semin. Liver Dis.* **19**, 129–140 (1999).

12. Sandler, N. G., Mentink-Kane, M. M., Cheever, A. W. & Wynn, T. A. Global gene expression profiles during acute pathogen-induced pulmonary inflammation reveal divergent roles for Th1 and Th2 responses in tissue repair. *J. Immunol.* **171**, 3655–67 (2003).

13. Martinez, F. O. & Gordon, S. The M1 and M2 paradigm of macrophage activation: time for reassessment. *F1000Prime Rep.* **6**, 13 (2014).

14. Mosser, D. M. & Edwards, J. P. Exploring the full spectrum of macrophage activation. *Nat. Rev. Immunol.* **8**, 958–969 (2008).

15. Shetty, S., Lalor, P. F. & Adams, D. H. Lymphocyte recruitment to the liver: molecular insights into the pathogenesis of liver injury and hepatitis. *Toxicology* **254**, 136–46 (2008).

16. Safadi, R. *et al.* Immune stimulation of hepatic fibrogenesis by CD8 cells and attenuation by transgenic interleukin-10 from hepatocytes. *Gastroenterology* **127**, 870–82 (2004).

17. Novobrantseva, T. I. *et al.* Attenuated liver fibrosis in the absence of B cells. *J. Clin. Invest.* **115**, 3072–3082 (2005).

18. Romagnani, S. T-cell subsets (Th1 versus Th2). *Ann. Allergy, Asthma Immunol.* **85**, 9–21 (2000).

19. Chiaramonte, M. G. *et al.* IL-13 is a key regulatory cytokine for Th2 cell-mediated pulmonary granuloma formation and IgE responses induced by Schistosoma mansoni eggs. *J. Immunol.* **162**, 920–30 (1999).

20. Chiaramonte, M. G., Donaldson, D. D., Cheever, A. W. & Wynn, T. A. An IL-13 inhibitor blocks the development of hepatic fibrosis during a T-helper type 2–dominated inflammatory response. *J. Clin. Invest.* **104**, 777–785 (1999).

21. McGaha, T. L. & Bona, C. A. Role of profibrogenic cytokines secreted by T cells in fibrotic processes in scleroderma. *Autoimmun. Rev.* **1**, 174–81 (2002).

22. Rodgarkia-Dara, C. *et al.* The activin axis in liver biology and disease. *Mutat. Res. Mutat. Res.* **613**, 123–137 (2006).

23. Schmierer, B. & Hill, C. S. TGFβ–SMAD signal transduction: molecular specificity and functional flexibility. *Nat. Rev. Mol. Cell Biol.* **8**, 970–982 (2007).

24. Thompson, T. B., Woodruff, T. K. & Jardetzky, T. S. Structures of an ActRIIB:activin A complex reveal a novel binding mode for TGF-beta ligand:receptor interactions. *EMBO J.* **22**, 1555–66 (2003).

25. Massagué, J., Blain, S. W. & Lo, R. S. TGFbeta signaling in growth control, cancer, and heritable disorders. *Cell* **103**, 295–309 (2000).

26. Tsuchida, K. *et al.* Activin isoforms signal through type I receptor serine/threonine kinase ALK7. *Mol. Cell. Endocrinol.* **220**, 59–65 (2004).

27. Doré, J. J. E. *et al.* Mechanisms of Transforming Growth Factor-β Receptor Endocytosis and Intracellular Sorting Differ between Fibroblasts and Epithelial Cells. *Mol. Biol. Cell* **12**, 675–684 (2001).

28. Runyan, C. E., Schnaper, H. W. & Poncelet, A.-C. The role of internalization in transforming growth factor beta1-induced Smad2 association with Smad anchor for receptor activation (SARA) and Smad2-dependent signaling in human mesangial cells. *J. Biol. Chem.* **280**, 8300–8 (2005).

29. Moustakas, A. Smad signalling network. *J. Cell Sci.* **115**, 3355–6 (2002).

30. Souchelnytskyi, S., Rönnstrand, L., Heldin, C. H. & ten Dijke, P. Phosphorylation of Smad signaling proteins by receptor serine/threonine kinases. *Methods Mol. Biol.* **124**, 107–20 (2001).

31. Harrison, C. A. *et al.* An Activin Mutant with Disrupted ALK4 Binding Blocks Signaling via Type II Receptors. *J. Biol. Chem.* **279**, 28036–28044 (2004).

32. Wang, S.-Y. *et al.* Inhibitory effect of activin A on activation of lipopolysaccharide-stimulated mouse macrophage RAW264.7 cells. *Cytokine* **42**, 85–91 (2008).

33. Ogawa, K., Funaba, M., Chen, Y. & Tsujimoto, M. Activin A functions as a Th2 cytokine in the promotion of the alternative activation of macrophages. *J. Immunol.* **177**, 6787–94 (2006).

34. Gold, E. J. *et al.* βA- and βC-activin, follistatin, activin receptor mRNA and βC-activin peptide expression during rat liver regeneration. *J. Mol. Endocrinol.* **34**, 505–515 (2005).

35. Wang, D.-H. *et al.* Role of activin A in carbon tetrachloride-induced acute liver injury. *World J. Gastroenterol.* **19**, 3802 (2013).

36. Gold, E. J. *et al.* Changes in activin and activin receptor subunit expression in rat liver during the development of CCl4-induced cirrhosis. *Mol. Cell. Endocrinol.* **201**, 143–53 (2003).

37. Zhang, H. *et al.* Adenovirus‐mediated knockdown of activin A receptor typeï¿½2A attenuates immune‐induced hepatic fibrosis in mice and inhibits interleukin‐17‐induced activation of primary hepatic stellate cells. *Int. J. Mol. Med.* **42**, 279–289 (2018).

38. Yndestad, A. *et al.* A Complex Role of Activin A in Non-Alcoholic Fatty Liver Disease. *Am. J. Gastroenterol.* **104**, 2196–2205 (2009).

39. Namwanje, M. & Brown, C. W. Activins and Inhibins: Roles in Development, Physiology, and Disease. *Cold Spring Harb. Perspect. Biol.* **8**, a021881 (2016).

40. Vejda, S. *et al.* Expression and dimerization of the rat activin subunits betaC and betaE: evidence for the ormation of novel activin dimers. *J. Mol. Endocrinol.* **28**, 137–48 (2002).

41. De Bleser, P. J., Niki, T., Xu, G., Rogiers, V. & Geerts, A. Localization and cellular sources of activins in normal and fibrotic rat liver. *Hepatology* **26**, 905–912 (1997).

42. Kreidl, E., Oztürk, D., Metzner, T., Berger, W. & Grusch, M. Activins and follistatins: Emerging roles in liver physiology and cancer. *World J. Hepatol.* **1**, 17 (2009).

43. Heymann, F., Hamesch, K., Weiskirchen, R. & Tacke, F. The concanavalin A model of acute hepatitis in mice. *Lab. Anim.* **49**, 12–20 (2015).

44. Kobayashi, T., Niimi, S., Fukuoka, M. & Hayakawa, T. Regulation of inhibin beta chains and follistatin mRNA levels during rat hepatocyte growth induced by the peroxisome proliferator di-n-butyl phthalate. *Biol. Pharm. Bull.* **25**, 1214–6 (2002).

45. Kanamori, Y. *et al.* Regulation of hepcidin expression by inflammation-induced activin B. *Sci. Rep.* **6**, 38702 (2016).

46. Wang, H.-X. *et al.* Immune mechanisms of Concanavalin A model of autoimmune hepatitis. *World J. Gastroenterol.* **18**, 119–25 (2012).

47. Erhardt, A., Biburger, M., Papadopoulos, T. & Tiegs, G. IL-10, regulatory T cells, and Kupffer cells mediate tolerance in concanavalin A-induced liver injury in mice. *Hepatology* **45**, 475–485 (2007).

48. Jones, K. L. *et al.* Activin A is a critical component of the inflammatory response, and its binding protein, follistatin, reduces mortality in endotoxemia. *Proc. Natl. Acad. Sci. U. S. A.* **104**, 16239–44 (2007).

49. Krueger, A., Fas, S. C., Baumann, S. & Krammer, P. H. The role of CD95 in the regulation of peripheral T-cell apoptosis. *Immunol. Rev.* **193**, 58–69 (2003).

50. Brunner, T. *et al.* Cell-autonomous Fas (CD95)/Fas-ligand interaction mediates activation-induced apoptosis in T-cell hybridomas. *Nature* **373**, 441–444 (1995).

51. Brenner, D., Krammer, P. H. & Arnold, R. Concepts of activated T cell death. *Crit. Rev. Oncol. Hematol.* **66**, 52–64 (2008).

52. Yaden, B. C. *et al.* Inhibition of Activin A Ameliorates Skeletal Muscle Injury and Rescues Contractile Properties by Inducing Efficient Remodeling in Female Mice. *Am. J. Pathol.* **184**, 1152–1166 (2014).

53. Mee Yang, Y. & Seki, E. TNFα in liver fibrosis. doi:10.1007/s40139-015-0093-z

54. Canbay, A. *et al.* Kupffer cell engulfment of apoptotic bodies stimulates death ligand and cytokine expression. *Hepatology* **38**, 1188–1198 (2003).

55. Connolly, M. K. *et al.* In liver fibrosis, dendritic cells govern hepatic inflammation in mice via TNF-α. *J. Clin. Invest.* **119**, 3213–25 (2009).

56. Chu, P. *et al.* C-C motif chemokine receptor 9 positive macrophages activate hepatic stellate cells and promote liver fibrosis in mice. *Hepatology* **58**, 337–350 (2013).

57. Liao, W., Lin, J.-X. & Leonard, W. J. IL-2 family cytokines: new insights into the complex roles of IL-2 as a broad regulator of T helper cell differentiation. *Curr. Opin. Immunol.* **23**, 598–604 (2011).

58. Bachmann, M. F. & Oxenius, A. Interleukin 2: from immunostimulation to immunoregulation and back again. *EMBO Rep.* **8**, 1142–8 (2007).

59. Weng, S.-Y. *et al.* IL-4 Receptor Alpha Signaling through Macrophages Differentially Regulates Liver Fibrosis Progression and Reversal. *EBioMedicine* **29**, 92–103 (2018).

60. Kalafateli, M., Konstantakis, C., Thomopoulos, K. & Triantos, C. Impact of muscle wasting on survival in patients with liver cirrhosis. *World J. Gastroenterol.* **21**, 7357–61 (2015).

61. Stepniak, E. *et al.* c-Jun/AP-1 controls liver regeneration by repressing p53/p21 and p38 MAPK activity. *Genes Dev.* **20**, 2306–2314 (2006).

62. Amanzada, A. *et al.* Myeloperoxidase and elastase are only expressed by neutrophils in normal and in inflamed liver. *Histochem. Cell Biol.* **135**, 305–15 (2011).

63. Mack, M. Inflammation and fibrosis. *Matrix Biol.* **68**–**69**, 106–121 (2018).

64. Rani, R., Tandon, A., Wang, J., Kumar, S. & Gandhi, C. R. Stellate Cells Orchestrate Concanavalin A–Induced Acute Liver Damage. *Am. J. Pathol.* **187**, 2008–2019 (2017).

65. Kudo, H. *et al.* Lipopolysaccharide triggered TNF-α-induced hepatocyte apoptosis in a murine non-alcoholic steatohepatitis model. *J. Hepatol.* **51**, 168–175 (2009).

66. Romagnani, S. Th1/Th2 cells. *Inflamm. Bowel Dis.* **5**, 285–94 (1999).

67. Nikolic-Paterson, D. J., Wang, S. & Lan, H. Y. Macrophages promote renal fibrosis through direct and indirect mechanisms. *Kidney Int. Suppl.* **4**, 34–38 (2014).

68. Braga, T. T., Agudelo, J. S. H. & Camara, N. O. S. Macrophages During the Fibrotic Process: M2 as Friend and Foe. *Front. Immunol.* **6**, 602 (2015).

69. Ebeid, H. M., Gibriel, A. A. Y., AL-Sayed, H. M. A., Elbehairy, S. A. & Motawe, E. H. Hepatoprotective and Antioxidant Effects of Wheat, Carrot, and Mango as Nutraceutical Agents against CCl_4 -Induced Hepatocellular Toxicity. *J. Am. Coll. Nutr.* **34**, 228–231 (2015).

70. Su, S.-B. *et al.* Mechanisms of CCl 4-induced liver fibrosis with combined transcriptomic and proteomic analysis. *J Toxicol. Sci.* **41**, 561-72 (2016).

71. Kubota, N. *et al.* A high-fat diet and multiple administration of carbon tetrachloride induces liver injury and pathological features associated with non-alcoholic steatohepatitis in mice. *Clin. Exp. Pharmacol. Physiol.* **40**, 422–430 (2013).